0 0 0 0 4 3 0 1 4 7 3

Submitted to Solar Energy

RECEIVED
LAWRENCE
RADIATION LABORATORY

MAR 17 1975

LIBRARY AND
DOCUMENTS SECTION

LBL-3672
Preprint c.1

THEORY AND PRINCIPLES OF LOW TEMPERATURE HOT AIR ENGINES FUELED BY SOLAR ENERGY

Dan Haneman

February 12, 1975

Prepared for the U. S. Atomic Energy Commission
under Contract W-7405-ENG-48

For Reference

Not to be taken from this room

LAWRENCE BERKELEY LABORATORY
UNIVERSITY OF CALIFORNIA
BERKELEY

LBL-3672
c.1

DISCLAIMER

This document was prepared as an account of work sponsored by the United States Government. While this document is believed to contain correct information, neither the United States Government nor any agency thereof, nor the Regents of the University of California, nor any of their employees, makes any warranty, express or implied, or assumes any legal responsibility for the accuracy, completeness, or usefulness of any information, apparatus, product, or process disclosed, or represents that its use would not infringe privately owned rights. Reference herein to any specific commercial product, process, or service by its trade name, trademark, manufacturer, or otherwise, does not necessarily constitute or imply its endorsement, recommendation, or favoring by the United States Government or any agency thereof, or the Regents of the University of California. The views and opinions of authors expressed herein do not necessarily state or reflect those of the United States Government or any agency thereof or the Regents of the University of California.

Theory and Principles of Low Temperature Hot Air Engines Fueled by Solar Energy

D. Haneman*

Laboratory of Chemical Biodynamics
Lawrence Berkeley Laboratory
University of California 94720

ABSTRACT

For heating uses, solar energy conversion systems are currently close to being economic. For power generation they are less so. A brief analysis of relevant points and system efficiencies is given. It is concluded that the most promising approach is a properly combined heat plus power generation assembly. Attention is focussed on low temperature flat plate collector systems since these are already demonstrably competitive in some areas. The low efficiencies of energy transducers based on these are acceptable if the heat they reject during operation is at sufficiently high temperature to be readily recycled or directly useful. The most effective methods using this principle are shown to be open cycle air engines. The principles of these are discussed and some practical design features are reported.

* Visiting Scientist, now at School of Physics, University of New South Wales, P.O. Box 1, Kensington, Australia 2033.

1. INTRODUCTION

There is considerable interest in the generation of mechanical and electrical power from solar energy. Most approaches involving large scale power production are based on transducers requiring high temperatures, which thus involve means of focusing the solar radiation. These require, in most designs, some form of tracking the sun's motion, and they also lose much of the diffuse part of the solar radiation. However, the high temperature operation does permit more efficient conversion of solar radiation to mechanical work, due to the Carnot principle. For an ideal engine working in a closed cycle, taking in heat at a high (Kelvin) temperature T_2 and rejecting it at a low temperature T_1, the maximum possible fraction of the input heat that can be converted to work $\eta_c = (1 - T_1/T_2)$. Thus if T_2 is only, say, 80°C, and T_1 is ambient temperature of say, 27°C, then the maximum thermal conversion efficiency $\eta_c = (1 - \frac{300}{353}) \approx 16\%$ which is low. Hence the interest in higher temperature operation.

There are, however, good reasons for considering low temperature operation as well.

Currently about 25% of U.S. oil consumption is devoted to heating and cooling of domestic dwellings [1]. The application of solar energy to such purposes has already been shown to be practical. It is also economic. Flat plate collectors, which use solar energy to heat water to temperatures up to about the boiling point, are already installed in many areas of the world (parts of Australia, Israel and U.S.A. among others) and are coming into increasing use as fuel costs rise. These often provide more hot water than can be used in some parts of the summer. The heat is also useable in absorption based cooling systems. Hence it is an attractive

proposition to consider the coupling of an energy converter to existing flat plate collector systems.

It is important to note that though the conversion efficiency in such systems may be low, say for example 5%, the remaining 95% need not be wasted. In some designs to be considered later (open cycle), the rejected portion of the thermal input is still high grade heat and can be usefully fed back into the heat circulation system to serve the primary purpose of the installation. It may also be used directly. Hence the converter system is not wasteful, and involves no costs in setting up solar collectors since it is only a parasite on existing systems.

Flat plate collector systems have been intensively investigated. They need no sun tracking arrangements, and collect diffuse as well as direct insolation (incident solar radiation). Costs will drop greatly with large scale use. The collection efficiency of some typical [1,2] commercially available flat plate collectors is shown in Fig. 1. Note that collection efficiencies of about 50% are feasible at useful temperatures.

Economics play a vital role in solar energy conversion systems. The problem is not how to convert, of which there are a multitude of methods (thermal expansion, photovoltaic, photochemical, thermoelectric, photosynthetic, etc.), but how to do it at a competitive cost. This matter has been widely discussed, e.g. [3,4] and references therein. In the systems of main concern here there are four principal advantages. Firstly, as already mentioned, they need involve no extra collection systems. Secondly, they involve no special materials (e.g. silicon or other semi-conductors, or alloys such as nitinol). Thirdly, and paramount, the reject heat is at high temperature, and is still directly useful. Fourthly, no cooling water is required.

2. SUMMARY OF CONVERSION SYSTEMS AND EFFICIENCIES

a) High Temperature Systems

Let us first consider the maximum possible efficiency of a solar energy conversion system. The surface temperature of the sun is about 6000 K [4]. Assuming a radiation collector on Earth to be perfectly insulated and free of significant radiation losses, it could get no hotter than 6000 K (this is irrespective of how much focussing is used -- a receptor surface cannot get hotter than the radiant source). If heat is discharged at an average Earth ambient of 300 K, then the maximum thermal-to-work conversion efficiency η_c is $(1 - \frac{300}{6000}) = 95\%$.

In practice, solar furnaces which heat small objects of a few cm^3 volume in vacuum, attain temperatures as high as 3000 K with difficulty, permitting $\eta_c = 90\%$ [4]. However, the overall efficiency of such systems is very much less due to the collection efficiency F_c being much less than 100%. If estimated ideal figures F_c of 70% are used, for temperatures of about 1000 K, one might hope for an overall efficiency $F_c\eta_c$ of $0.7 \times 0.7 = 50\%$. Since, however, the ideal Carnot efficiency η_c is not attained, and taking into account various other losses in a real system, one would probably be fortunate to have an overall efficiency of about 30-40%. To date complete such systems have not yet been described with well documented efficiency figures. Presumably the figure of about 30-40% could be attained in a well designed and constructed assembly (of high cost).

b) Silicon Photovoltaic Cells

Such cells are practical long lived devices [4,5] which are in commercial production, currently costing about \$0.30 per cm^2 of area and about \$30 per "peak watt", i.e. per watt output from an assembly assuming peak solar radiation density to be present, approximately IKW m^{-2}. Although these

approximate costs are much less than those of the earlier cells supplied for space vehicle use, they are still too high to be competitive except in special applications. Thus in one year a $30 cell assembly yields 2KWH, worth about $0.04. However they are used for space vehicles and for unattended sites such as oil rigs where warning lights are needed and a reliable power source not needing occasional attention is required. There are also some other applications (some based on the novelty appeal).

Practical efficiencies of such devices range from 12 to 15% and hopes for reaching 20% have been mentioned. The figure refers to the ratio of (d.c.) electric power output to incident solar power. There are currently intense efforts to lower costs by using polycrystalline thin film rather than single crystal silicon, and also to produce the latter in sheet form. While success in such efforts is being attained, the prospects for large price reductions are still doubtful. In addition, there may be silicon supply problems for large scale use.

Each silicon cell provides about 0.5 V at about 25 mA per cm^2 at sunlight of 1 KWm^{-2}. The cells can be made large (discs of diameter 2.2 inches are commercially available) and connected in series to provide convenient voltages such as 12 V [6]. However, too many in series causes undesirable losses in the series resistance of the cells. Nevertheless the cells are long lived, have no moving parts, and are virtually maintenance free.

The theory of these devices has been worked out in detail using semiconductor theory [7]. It is useful to point out that they can also be discussed in the same framework as other thermal convertors, by reference to the Carnot principle. The incident radiation excites electrons from the valence into the conduction band, as in Fig. 2. The states left vacant in the valence band are referred to as "holes" and behave as though they are carriers having a positive charge. The presence of an inbuilt electric

field due to charged surface states (in surface barrier devices) or to controlled impurity gradients (in p-n junction devices) separates the conduction electrons and valence holes since they have opposite charges. They are thus prevented from recombining until they reach the specimen contacts, and then they recombine in the external circuit, giving out energy.

From a thermal point of view, the electrons excited into the conduction band are now "hot", i.e. their average energy is much higher than that of the electrons which are in thermal equilibrium with the vibrating ion cores of the material. This population of hot electrons can be regarded as having an average temperature T_2. The definition of T_2 requires care for particular cases, since the density of states in the bottom of the conduction band will affect the shape of the energy distribution which will not necessarily be Maxwellian. In a quantitative discussion, the distribution may be considered as an appropriate sum of Maxwellian distributions, each with its properly defined temperature, T_α, T_β, etc. The hot electrons subsequently give up energy and return to their thermal equilibrium states characterized by the temperature T_1. Hence the maximum efficiency of a photovoltaic cell is, in the usual way, $(1 - \frac{T_1}{T_2})$ or, as a refinement,

$$[n_\alpha(1 - \frac{T_\alpha}{T_2}) + n_\beta (1 - \frac{T_\beta}{T_2}) + \ . \ . \ . \ ]/(n_\alpha + n_\beta + \ . \ . \ )$$

where n_α hot electrons have an average temperature T_α, etc. The theoretical values of T_α etc. are thousands of degrees but the net solar efficiency is low because only a fraction of the insolation is used for electron excitation (the rest excites phonons, i.e. lattice vibrations), and there are also unavoidable conductive energy losses in the semiconductor. This discussion is given in order to put photovoltaic devices into the same thermal conversion efficienty framework as other converters such as engines. Other devices

mentioned briefly are:

i) Photochemical generators such as iron-thionine systems [8].

ii) Photon stimulated gas dissociation followed by catalysed recombination -- starting gases include SO_3, $COCl_2$ and NF_3 [9]. Also breakdown of water to produce hydrogen and oxygen [10].

iii) Other photovoltaic cell systems such as copper sulphide - cadmium sulphide [11].

iv) Thermoelectric devices [12].

v) Photoelectric emission devices (studied by the author, unpublished).

None of these are competitive in reliability and efficiency with the silicon cells at this stage.

This summary is confined to electric power or work generation, and not to means of deriving energy from sunlight such as plant growth, nor to wind power related to sunlight induced air movements, etc.

c) Engines

We now mention true engines, all based on certain parts getting heated, changing their dimensions and doing work. Heat is taken in, work done, and the unused heat rejected to some kind of sink, usually cooling water or air.

i) Engines based on thermal expansion of metals. Such expansion is normally very small but there is a large effect in a certain alloy known as nitinol. Advantage has been taken of this effect to design an engine using hot water as the energy source and cold water as the energy sink [13]. Much research is under way to make this a viable and efficient system. However, the fraction of input heat which is not used for useful work and is rejected to the cold sink, appears to be lost to the cold water. Hard estimates of the efficiencies so far attained are not available.

ii) Engines based on the expansion of externally heated gases, usually air. The best known example is the Stirling engine based on the Stirling cycle. Such engines afford a good example of how sufficient research and development can improve the efficiency. Most small Stirling or similar hot air engines have efficiencies of only a few percent at T_2 (high temperature) of about 700°C (η_c = 70%). However, an intense effort by the Philips Co. of Holland developed engines that have over 50% of the Carnot efficiency [14].

Such engines function well at temperatures of several hundred degrees Centigrade and must therefore be used with tracking focussed collectors. They are not effective at relatively low temperatures, as presently designed. This may be due to the regenerator not performing its function well at such temperatures. Since the Stirling cycle has a theoretical ideal efficiency equal to that of the Carnot, it may well be worthwhile to consider adapting the design for low temperature use, by using a longer regenerator section, for example, and thus taking advantage of available flat plate collectors. However, effective cooling is essential in the Stirling cycle and thus the rejected heat would be lost to the cooling medium. We discuss this point later.

Other closed cycle hot air engines have been built but none appear to have been developed to the same degree as the Stirling engine.

iii) Internal combustion engines. These are extensively treated in textbooks on engineering thermodynamics. Well known examples are those based on the Otto cycle (internal combustion motor car engines), the diesel cycle, the Joule or Brayton cycle (currently used in turbines), and Sargent cycle. Currently efficiencies of about 70% of the theoretical Carnot value can be attained in high temperature operation. However low (∿100°C) temperature applications have been very little investigated.

iv) Rankine cycle engines based on expansion of a heated vapour and condensation back to liquid in the heat rejection phase. This cycle is extensively employed in steam engines and they form the subject of a thorough research and development effort [15].

For solar energy use, Rankine cycle engines operating between about 95°C and 35°C have been built, using organic fluids of suitable boiling points and condensation temperatures [16-19]. Efficiencies approaching 70% of the Carnot value for these temperatures have been reported [16]. (Here efficiency means turbine shaft power divided by heat input to the working fluid.) Hence they are suitable for use with flat plate collectors.

d) Combined Flat Plate Collector and Engine Systems

We now consider the total efficiency to be expected from the above combination.

The overall efficiency η_o depends on the efficiency F_c of the flat plate collector system and on the convertor,

$$\eta_o = F_c \eta_e$$

where η_e is the net efficiency of the thermal convertor. The maximum value of η_e is η_c, the Carnot efficiency. Although η_c rises with temperature, F_c falls, as shown in Fig. 1, since radiative and conductive losses of the collector increase as its equilibrium temperature increases.

In Fig. 3 we plot $\eta_o = F_c \eta_e$, using the values of F_c from Fig. 1. Note that the maximum overall efficiency for the combination occurs when the exit water temperature from the collector is in the region of 90°C. Furthermore, the maximum of η_o is approximately 8%. The key questions then are 1) What efficiency can be achieved in practice, 2) What costs are involved. We consider these points in turn.

The Rankine cycle engine, as mentioned in section c(iv) above, has already been developed to the stage where about 70% of the Carnot

efficiency is obtainable in the low temperature as well as high temperature region of operation. No other engines have as yet been seriously developed in the low temperature region. Presumably equal success could, however, be obtainable. We therefore assume that about 60% of the theoretical maximum 8% efficiency of the combination is available, i.e. approximately 5%.

We now consider cost requirements. A normal flat plate collector system for an average domestic installation would have an area of about $3m^2$. The total insolation in one year in a region of good sunshine, e.g. southern U.S.A., is about 2000 KW hours per m^2. Therefore 6000 KWH is collected, and 5% used for work gives 300 KWH. This would reduce electric power consumption correspondingly; the incremental cost of the latter varies but we take an average figure of 2 cents per KWH. Hence the saving is $6 per annum for work. Assuming that the total cost of the unit should not exceed about 5 times the annual saving, one requires a cost of about $30. This figure applies to the engine. It is assumed that the flat plate collector system is already cost justified because of the hot water it supplies.

It may seem that $6 of electricity per annum is not worth bothering about. However, on a daily basis there are additional considerations. The engine power from $3m^2$ during peak insolation is 5/100 x 3 KW = 150 watts. This is readily sufficient to drive the pump that is usually installed to circulate the hot water (or water mixture) through the collector -- most pumps use about 50 watts. In an easily designed installation, the engine drives the pump directly, without using a generator or electric motor. Not only is such a system optimized, but it makes it independent of electricity supplies which is a highly desirable feature. One does not want a solar collector installation to cease functioning if there is an electric power failure (strike, breakdown, civil emergency, etc.)

One could take the view that the above application is in itself worthwhile and that the sole use of the engine in a small domestic installation be for direct drive of the fluid circulating pumps, both in the collector system, the refrigeration fluid circuit and if necessary in the direct hot water supply to the household. No generator or power storage system is then required, since the engine output is not sufficient to justify the costs and problems of battery provision. There is then some further cost saving in that only a smaller, less durable electric motor need be provided for the pumps, intended as a short run emergency unit only.

In further considering costs, it is necessary to distinguish between small distributed domestic systems and large central supply installations.

i) Domestic systems.

As shown above, a cost of about $30 is required for an engine of output up to 150 watts, on normal economic considerations. This figure seems difficult to achieve. Justification for use of such a system would be based more on the advantages of driving the fluid pumps by solar energy, thus achieving independence from electricity supplies during sunlight hours.

There is another consideration. The engine, in attaining about 9% efficiency (against a Carnot figure of about 14%) is rejecting 91% of the input heat to it. If a condensation type engine (Rankine cycle) is being used, it is essential to cool the condenser to at least about 35°C, depending on the fluid, to attain the above efficiencies. If cooling water is used, its exit temperature from the engine will then be in the vicinity of 30°C or less, depending on the flow rate. This warm water is at too low a temperature to be useful except in a few non-general applications. Furthermore, it is not practical to recycle it through the solar flat plate collector since simple calculations show that the flow rate is too large for it to become hot enough to power the input of the engine.

A practical figure is obtainable from the operation of the high efficiency Prigmore-Barber engine [16]. It obtains input heat from 11 gpm of 215°F (100.7°C) water but requires more than twice this flow rate, 25 gpm, of 85°F (29.5°C) cooling water. Since the major part of the slightly warmed cooling water could thus not be recycled, and is of little other use, a corresponding fraction of the heat collected by the collector is wasted. Furthermore, most domestic systems cannot function satisfactorily by constantly running cool water into the collector since the demand is not continuous. Operation of current practical collectors is based on a closed loop recycling system where the input temperature to the collector is well above 100°F when high exit temperatures are achieved.

The above consideration shows that the economics of installing a flat plate collector system for hot water production would be seriously disturbed by attachment of a low efficiency engine whose cycle requires cooling to near ambient temperature. There would be considerable waste of heat since the engine's reject heat is at a low temperature and not generally useful. Hence the economics of the system, already doubtful as far as the cost of the engine alone, would be such as to throw the flat plate collector system itself into jeopardy.

ii) Large central installations.

Here one uses a large area collector. Most designs envisage some form of solar (Tabor) bond as the only practical low cost method [20]. These have not as yet been used in any widespread way as have rooftop flat plate collectors, and costs are thus more difficult to estimate. Although hard cost figures are not obtainable even optimistic estimates make the use of a large Rankine cycle powered generator in conjunction with the pond, a marginal proposition at present. It appears at least highly desirable, and probably essential, to keep the reject heat from the engine at a

sufficiently high temperature to be generally useful. (Special uses for slightly warm water are in crop growth and sewage treatment but these are not general.) We now discuss ways of handling this problem.

3. OPEN CYCLE LOW TEMPERATURE ENGINES

We will not detail here the advantages of low temperature collectors -- as has been implicitly assumed, their spreading use is proof of their practicality. Hence, as mentioned about, it is realistic to consider parasite engine attachments to such systems, provided the engine does not waste heat energy that would otherwise be used for heating purposes. Thus the collector is kept economic in its own right as a source of hot water (used also for absorption refrigeration systems).

As shown above, engine cycles using a condensing vapour must reject heat at a fairly low temperature. (If a higher condensation temperature T_1 is used, efficiency falls since the efficiency numerator is proportional to $(T_2 - T_1)$. Hence the reject heat is at too low a temperature to be generally useful. We now consider engine cycles which overcome this difficulty.

We refer to Fig. 4 which shows several ideal (air standard) engine and TS cycles on the PV and TS planes. The heat rejection stage is c-d. Clearly the optimum effect for our purposes is to take the heat out at point c, where it is at the maximum temperature after the work stroke. However this can only be achieved by removing the hot working fluid directly from the engine. If any heat transfer process is used, the coolant starts at temperature say T_c which must be less than T_1, and heats up to T_1 while the working fluid cools to T_1.

If the fluid is removed, and new fluid is injected at ambient temperature from some stored source, one has a so called open cycle. This is

effectively what occurs in internal combustion engines where the heated gas is ejected (and usually wasted) and a new charge of air plus fuel is injected. It is usual to analyze such cycles as though they were closed, since the situation is equivalent to the charge being cooled and restored to its pre-explosion condition.

A Rankine cycle could operate on open cycle if the hot fluid were ejected after the work stroke, and fresh fluid were supplied. This has been used in steam engines where the spent steam has other industrial applications and water is cheap. However in low temperature engines the fluids are too expensive, and in any case are usually noxious and/or inflammable to varying degrees. Thus the fluid must be in a sealed system and in fact prevention of leaks in the assembly is a critical design requirement, due to the high leak rate of such fluids.

Clearly only air can be used economically in open cycle low temperature engines. The hot air is ejected at T_3 and fresh air drawn in at T_1 from an essentially unlimited supply. Hence we consider open cycle low temperature air engines.

a) Theory

i) The Lenoir cycle. The simplest system consists of heating a mass of air which then does work when it expands. Afterwards the air is cooled, or ejected and replaced. This system was used (at high temperatures) by Lenoir in 1860. The efficiency was found to be too low. The ideal cycle is illustrated in Fig. 5. It is sometimes drawn as only the triangular section A above the ambient pressure line, and described as having no compression.

It is pointed out that such a description is not strictly correct. After expansion to ambient pressure, the air would cool, at constant volume, to ambient temperature. This causes its pressure to drop below

ambient pressure. Then work is done by the ambient pressure in compressing the gas back to its starting volume. This is illustrated in Fig. 5. Note that the full cycle A plus B is then similar to an Otto cycle.

The Lenoir cycle has the advantage of simplicity since one only needs to heat a mass of air in a box, either by direct solar radiation or via hot water. If it is adapted to open cycle use then the air, heated from T_1 to T_2 by fuel (solar energy), is ejected after doing work in the expansion stroke, and a new charge of air is taken in. In this case only the portion A of the PV cycle is involved. Furthermore the expansion stroke need not be a single large one, inconvenient in practice, but be composed of many short ones if a convenient reciprocating piston expander is used. Thus the piston in a cylinder is forced out, an inlet valve closes off the air reservoir while the piston returns, expelling the air in the cylinder through an exhaust valve, and the inlet valve reopens while the exhaust valve shuts. Then air from the reservoir pushes out the piston again in a new work stroke. This stepped open cycle, or "hemi cycle" is shown in Fig. 5 on the R.H.S. The equivalent work cycle is very similar to that of a single large expansion, as shown.

The efficiencies for these cycles are readily calculated and the formulae and temperature variations shown in Fig. 6. For illustration, the efficiency η_A of the open A cycle is shown, and the difference between this and the full, closed Lenoir cycle, is shown separately as η_B. Note that η_A is not much larger than η_B. This indicates that the open cycle efficiency is only a little more than half that of the closed cycle, $(\eta_A + \eta_B)$, particularly at low temperatures ($T_2/T_1 \sim 1.1$). By comparison with the Carnot efficiency η_c, the theoretical open cycle Lenoir efficiency η_A is seen to be only about $\eta_c/6$, and of course a practical value would be even lower.

Although the efficiency is very low, the important feature is whether the cost of a system can be made low enough to compensate. Note that the poorer the efficiency of an open cycle, the higher the temperature of reject heat since less heat has been converted in the cycle. If the reject heat is useable then the low efficiency is only of concern as imposing more severe restrictions on the allowable cost of the converter.

ii) The Otto cycle. The air standard Otto cycle is shown in Fig. 4. Note that the fluid is first compressed adiabatically, thereby rising in temperature from T_1 to $T_{1'}$. It is then heated to T_2. Hence $T_{1'}$ must obviously be less than the temperature T_2 which for solar operation is about 80-100°C. This limit on $T_{1'}$ limits the allowable compression and hence the theoretical efficiency. In an ideal Otto cycle, the efficiency $\eta_{Otto} = 1 - T_1/T_{1'}$. Note that if $T_{1'}$ is very close to T_2 then η_{Otto} approaches $1 - T_1/T_2$ which is the Carnot efficiency. However, the closer $T_{1'}$ approaches T_2, the slower the heat transfer that can take place due to the smaller temperature difference. Furthermore, referring to the diagram, it is easy to show that

$$T_1/T_{1'} = T_3/T_2 = \left(\frac{V_2}{V_1}\right)^{\gamma-1}$$

where volume V_1 is compressed to V_2 and γ is the ratio of specific heats at constant pressure and constant volume. Hence for a given starting temperature T_1, and a limited range for T_2, then the higher $T_{1'}$, the lower is T_3. If one is considering open cycle operation one does not want T_3, the temperature of the emitted fluid (air) to be too low as described above, lest it be useless. Hence there are various conflicting factors whose combination needs to be optimised in determining what compression ratio is theoretically desirable. The requirements are to

1) maximize $T_2-T_{1'}$ for optimum heat transfer

2) minimize T_2-$T_{1'}$ for maximum theoretical efficiency

3) set a minimum acceptable value on T_3 consistent with a value of T_2 that is optimum for solar collector performance.

In Fig. 7 we plot T_3 versus inverse compression ratio V_2/V_1 for different values of T_2, using γ = 1.4 which is approximately correct for air. A typical satisfactory combination could be T_2 = 360K (∿ 87°C), T_3 = 330K (∿ 57°C), $T_{1'}$ = 327K and T_1 = 300K, giving a compression ratio of 5:4 and a theoretical cycle efficiency of 8.25%. The Carnot cycle would give 16.7%. The upper temperature T_2 of 87°C is satisfactorily within the optimum range for a collector-engine assembly discussed in section 2(d), and the exhaust temperature T_3 of 57°C is sufficiently high for a variety of direct heating purposes, or for heating water for recycling into the collector.

iii) Diesel and Brayton Cycles. The ideal diesel and Joule-Brayton cycles are illustrated in Fig. 4 on the pressure-volume plane. The significant difference from the Otto cycle occurs in section b-c, since work is done as soon as heat enters the fluid, the pressure remaining (ideally) constant. Hence the temperature of the fluid remains near $T_{1'}$, which optimizes the heat transfer from the solar heated source (hot metal) at the higher temperature of about T_2. In the Otto cycle on the other hand, the fluid temperature rises towards T_2 <u>before</u> a work stroke is permitted. Hence the rate of heat transfer diminishes as the temperature rises.

Since the work done is proportional to the area of the closed PV cycle (or psuedo closed in the case of an open cycle), the Otto and Brayton cycles are somewhat more efficient than the diesel cycle. However, the approach of point d in the Brayton cycle to the initial pressure, is achieved using a turbine or other device which does work at very little thrust. In the relatively low temperature-low maximum thrust regimen being considered here, the point d would tend to lie above the starting pressure line, thus reducing

the efficiency below that of the Otto cycle.

Clearly a compromise must be chosen between maximum heat transfer to the fluid and maximum efficiency of the cycle. The first factor is of less importance in internal combustion engines, but is critical in low temperature solar engines. The sequence goes:

Lenoir cycle:	Heat transfer maximum.	Efficiency minimum.
Otto cycle:	Heat transfer minimum.	Efficiency maximum.
Joule-Brayton cycle:	Heat transfer intermediate.	Efficiency intermediate.
Diesel cycle:	Heat transfer intermediate.	Efficiency intermediate.

The optimum choice depends on various practical features which we now consider.

b) Practice

i) Heat transfer. It is well known that heat transfer is slow if the temperature difference is small, and extensive engineering tables on this subject are available. In considering low temperature solar engines, one may choose to transfer heat from solar heated water to the air in the engine, or else expose the air directly to solar radiation.

Direct heating units have been developed, e.g. [21], in which solar radiation passing through the glass windows of a type of flat plate collector, impinged on a honeycomb array of blackened slotted aluminum sheets. A temperature rise of 50 C° could be obtained with an airflow of 3 $ft^3 min^{-1}$ in bright sunlight. If the direct insolation is to be effectively used, a very fast rate of air flow, or engine open cycle turnover, is required to carry it away, due to the low thermal capacity of air compared to water.

Consider a flat collector of area A exposed to normally incident solar radiation of rate Q joules in t seconds. Let the height of the box be h, and c_v the specific heat (constant volume) of air be taken as 0.172 cal/gm°C. Then the heat required to raise the temperature of the air in the box by T is

$$Q = \rho A h c_v T$$

where ρ is the density of air, approximately 1.3 gm/litre. Taking T as 50 C°,

$$Q = 47.7 \times 10^3 \text{ joules}$$

If the insolation has its peak value of 1000 watts/m^2, then the time required to heat the air in the box is

$$t = Q/(1000\ A) \text{ sec} = 47.7\ h \text{ sec}$$

where h is in meters. For a box of height 1/6 meter (typical), the heating time is about 8 seconds. Assuming a collector efficiency F_c of about 50%, one obtains a time of 16 seconds; this collector efficiency implies a heat transfer to the air that is as effective as to the water in the standard flat plate collector. Hence it is necessary to have an air throughput of Ah m^3 in about $48hF_c$ seconds,

$$\text{Flow} = A/48F_c\ m^3s^{-1}$$

where A is in square meters. For a $3m^2$ area domestic installation, a flow of about 0.03 m^3s^{-1} is required, which implies a correspondingly high displacement for an engine, about 1.1 ft^3s^{-1} during peak insolation. Note that the rate is independent of the height of the box (to first order).

The above peak displacement rate is high, but achievable. If, however, the heat input to the engine fluid is from stored hot water, then the engine can work for 24 hours per day rather than being required to utilize all the insolation during the 6-8 hours per day of its maximum value. Thus a lower and more convenient displacement rate, of 0.5 ft^3s^{-1} or less, is allowable.

The above has assumed a heat transfer rate to the air that is as effective as that in a water cooled flat plate collector. The date mentioned above of 3 ft^3min^{-1} air flow rate for a 50 C° temperature rise [21], indicates a heat removal that is about 1/20 of that required, namely 66 ft^3min^{-1}. Similar results were obtained in experiments we performed using a very inexpensive heat transfer material.

Scrap lathe turnings were blackened by 3 methods: 1. Black spray paint (expensive); 2. Torching with an acetylene flame; 3. Placing a pile of turnings over cotton soaked in toluene and ignited. Of these, method 2 was the most useful. A flat plate collector box with a single plastic sheet window was filled with the turnings, the measured parts of which attained an equilibrium temperature of 120°C , and maintained about 87 C° when air at about 10 ft^3min^{-1} was blown through the box. The exit temperature of the air was 78°C , (about 50 C° above ambient). (Improved results would be obtainable with a 2 glass window collector) However this method is not favoured for engine application since power is wasted in forcing air through the collector.

It appears better to extract heat from hot water for 3 reasons: 1. Standard water cooled flat plate collectors can be used; 2. Less energy is required to pump liquid through the collector than to blow air at sufficient rates; 3. Stored heat in water can be used to operate the engine at night and on overcast days, thus lengthening the work time and reducing the displacement needed for the engine.

We consider utilization of the heat in the hot air expelled in the open cycle exhaust phase. For space heating purposes the air can be fed directly into the necessary regions with the usual fan assisted ducting. However, some of the heat, at least some of the time, might be better utilized by returning it to the primary closed loop water system in the solar collector, or to the secondary hot water storage system. This needs an effective air to water heat transfer system, perhaps based on a car radiator design (operated for reverse purpose).

ii) Compression. As described above, greater engine cycle efficiency is obtainable if compression above atmospheric pressure is used. The corresponding temperature rise should be appreciably less than that required

to attain T_2, otherwise excessive heat transfer times are involved. In section a)ii), it was concluded that a reasonable operation cycle involved a compression (volume) ratio of about 5:4. This would increase the pressure by about 9%, or about 1.3 lb in^{-2}. This is slightly beyond the pressure reached by fan type compressors. The latter are also rather inefficient, although inexpensive. Rotating vane or reciprocating piston type compressors readily attain such pressures; usual commercial types are designed for rather higher pressures. They are also somewhat inefficient (60-90%), both because of power losses in the electric drive motor (if one is used), and through leakage in valves, and past the vane or piston, and also through wasted heat generation in the compressor chamber.

For these reasons alone, care in considering the use of compression cycles is necessary. An additional point of concern is leakage in the fluid storage chamber in which the fluid is compressed, since storage must be long enough for sufficient heat transfer to take place (portion b-c of the P-V cycles in Fig. 4).

iii) High Pressure Flat Plate Collector. Some trials were carried out with storage chambers involving heating of the air by masses of blackened lathe turnings exposed to sunlight. Even in a Lenoir cycle, the pressure of a sun-heated sealed air volume can rise by about 10%. In a normal flat plate collector, this causes pressures of about 1.5 lb in^{-2} on the inner glass window, which would crack a single 4' x 2' sheet of 1/8" glass, whether normal glass or strengthened. From tables of glass sheet specifications, it was decided that 2' x 1' panes of normal glass, 1/4" thick, should withstand the pressure. It is desirable to use normal glass since tempered glass is expensive, often has inconvenient delivery times, and cannot be cut or modified after tempering.

The construction of the high pressure flat plate collector is shown in Fig. 8. A plastic sheet was pressed against the 4 glass panes, thereby preventing air leaks at the edges where they were in contact. These regions were also covered by supporting timber cross members as shown. Although 3/4" thick plywood was used for the box, with glue between the plys, it was found that air leaked readily through the first ply, along the glue plane, under the box side walls, and out. It was necessary to paint the inside of the box with three coats of epoxy to stop detectable leaks of this kind. The glass window edges were held down by angle iron segments, and rubber bead seals used all round. These precautions reduced leakages greatly, but nevertheless a leakage remained, corresponding to a pressure drop rate of about .036 lb in^{-2} per minute, at a pressure of 1 lb in^{-2}. The box did withstand $1\frac{1}{2}$ lb in^{-2} pressure, as required, and was of relatively simple and inexpensive construction. In order to overcome the effects of the small remanent leak rate, a sufficiently high heat transfer rate and work cycle rate would have to be used. It was concluded, although tentatively, that a better overall approach might be to use a sealed metal drum as the pressure storage chamber and transfer heat into the stored fluid by running solar heated water through it. This gives the additional benefit mentioned earlier, that normal flat plate collectors can be used and the solar heat can be stored in the water for use at any convenient time.

iv) Engine-Compressor Design. Because of the unsatisfactory efficiencies of commercial air compressors for low pressure solar application, a compressor-engine assembly was constructed specifically for the purpose. To minimize losses, a reciprocating piston type was used. Brass tubes of 3" diameter were chromium plated on the inside and fitted with aluminum

pistons coated externally with teflon. The 1-1/2" long piston cups were fitted with steel push rods using a simple hinge. Mass in the moving assembly was minimized.

To reduce air leaks in the valves, and also to reduce work losses in opening the valves against pressure, sliding types were used. A picture of the assembly is shown in Fig. 9. The exhaust valve in partly open position is seen, consisting of an aluminum cylinder fitting neatly over slots in the brass cylinder wall, just in front of the inlet valve which is internal and not visible. This valve was of a similar design. Excellent results were achieved for it using a shortened slotted syringe body and internal plunger. The two valves were activated by a lever L which was pushed by a rod whose other end slid on the piston rod using a teflon bearing B. Valve timing was readily adjusted by moving the stops on the piston rod which bore against B during the stroking.

To minimize parts, the two compressor cylinders were made to also act as engines. A falling weight system rotated the pulley seen on the RHS of the photo, which drove the pistons and thus pumped up the collector box. Sun derived heat further increased the pressure. A simple changeover lever situated between the cylinder then reversed the actions of the valves in the two cylinders, thus converting them to engines. The pressure in the box was then used to thrust the pistons and rotate the pulley, raising the weight system again and doing extra work.

The above operation is a staggered open Otto cycle. Air is compressed, heated, expands doing work and is then exhausted to the atmosphere. The compression and work-exhaust strokes are staggered into a number of small strokes, thus avoiding use of a single large cylinder and piston, or else a narrow cylinder with an extremely long stroke, either of which are inconvenient.

Experience with the above assembly, which withstood weathering well, led to several conclusions. The teflon coated piston in the chrome plated cylinder was effective in virtually eliminating appreciable leaks without the use of lubrication. (The latter in fact caused binding.) The sliding valve system operated on very low pressures and the inlet valve syringe assembly was sufficiently leak tight. However, the exhaust valve (outer cylinder slots) was less effective due to a less perfect sliding fit, and required modification. The engine cylinder could operate the 5 lb flywheel on a drive pressure as low as 0.036 lb in^{-2} (1" water head, or 2.5 gm cm^{-2}), giving 18 rpm. This gives an indication of the great reduction in friction losses since the piston area was approximately 6 in^2, giving a thrust of approximately 0.2 lb wt. and a torque at the flywheel of .025 lb in (2.5 in. piston stroke, $1\frac{1}{4}$ in. crank length). However, the permanent slight leak rate remaining in the storage box was sufficiently great to seriously affect the pressure rise due to solar heating of the air. In addition, the dead volume in the valve system at the end of the compression stroke needed to be reduced.

For the latter reasons it was concluded that the above approach, to be successful, required further refinement. Alternative techniques seemed well worth study. These would avoid the usual elements of a compressor, vanes and pistons, altogether. Instead, advantage would be taken of the relatively low compression needed in a solar hot air cycle, namely about 5:4 [section a)ii)]. This allows use of an elastic membrane permanently sealed over the storage reservoir. Such membranes can readily be stretched inward by an amount needed to achieve the necessary compression, using a variety of possible mechanisms. Heat transfer to the compressed air can be achieved by running solar heated water through pipes threading the storage volume, or spraying the water in directly. The latter results

in some water vapour loss during open cycle exhaust but the large surface area of the multitudinous drops promotes rapid and effective heat transfer. Trials indicated that 90°C water applied over a wettable porous area of 3 in^2 surrounding an air volume of about 2 in^3, caused heating to close to the water temperature in less than 1 second.

Experimentation along the above lines can follow several paths and finding the best method involves appreciable research and development, comparable with that applied to other systems such as low temperature Rankine cycle engines and higher temperature hot air systems such as Stirling engines. In view of the points described in this paper, such effort appears well worthwile.

4. CONCLUSION

One practical economic approach to solar power generation is the fitting of parasite thermal engines to flat plate or solar pond collector systems that are cost justified in their own right as producers of hot water. It is important that the reject heat from the engine be at a sufficient temperature for recycling or direct usage, so as not to affect the economics of the collector system. Open cycle hot air engines seem to satisfy this requirement best. The theory of such engines suggests using a compression of about 5:4 for the present application, in an Otto or Brayton cycle. Some practical experience with high pressure flat plate collectors and staggered reciprocating piston compressor-engine designs is reported. Research is required on establishing the optimum methods of rapid low temperature heat transfer and minimum loss compression in order to realize the advantages of the approach. The advantages include 1) effective use of all input energy, 2) no special materials required, 3) no extra collector systems required, and 4) no cooling water necessary.

Acknowledgement

Useful discussions on thermodynamic cycles were had with Dr. M. Klein, A. Robertson and S. Kohler. The high pressure collector was constructed by R. O'Brien and the engine by V. Wray. Dr. J. Day of Lawrence Livermore Laboratory supplied information on current engine developments.

REFERENCES

1. R. W. Vernon and F. W. Simon, "Flat Plate Collector Performance determined experimentally with a Solar Collector". NASA Technical Memorandum TM X-71602, 1974.
2. PPG Industries, Inc., "PPG Prototype Baseline Solar Collector", (Pittsburgh, Pennsylvania 15222), 1974.
3. R. Ramakumar, H. Allison, W. Hughes, "Prospects for Tapping Solar Energy on a Large Scale", Solar Energy 16, 107-115, 1974.
4. F. Daniels, "Direct Use of the Sun's Energy", Ballantine Books, New York, 1974.
5. C. Pfeiffer, P. Schoffer, B. G. Spoos and J. A. Duffie, "Performance of Silicon Solar Cells at High Levels of Solar Radiation", Trans. Am. Soc. Mech. Eng. 84A:33, 1962.
6. e.g., Solar Power Corporation, Mass. 02184.
7. D. H. Seib and L. W. Aukerman, "Photodetectors", Adv. in Electronics and Electron Physics 34, 95-222, Academic Press, N.Y., 1973.
8. e.g., L. J. Heidt, "Photochemistry in the Liquid and Solid States", New York, Wiley, 1960.
9. R. J. Marcus, "Survey of Electron Transfer Spectra of Inorganic Ions", Solar Energy 4, 20-23, 1960.

10. A. Fujishima and K. Honda, "Electrochemical Photolysis of Water at a Semiconductor Electrode", Nature 238, 37-38, 1972.

11. "Developments in Photovoltaic Solar Energy Conversion for Earth Surface Applications", in United Nations Conference on New Sources of Energy, 35-S44, 35-S40, 35-S56, 35-S106, Rome, 1961.

12. V. A. Baum, K. Katz, ibid, E35Gr-S10, E35-S12.

13. Lawrence Berkeley Laboratory, "Nitinol Engine Project", EE Annual Report UCID 3706.

14. R. Walker, "Stirling Engines", Scientific American, August 1973.

15. "Steam - Its Generation and Uses", The Babcock and Wilcox Co., New York, 1963.

16. D. R. Prigmore and R. E. Barber, "A Prototype Solar Powered, Rankine Cycle System Providing Residential Air conditioning and Electricity", 9th Conference Proc. IECEC 326-333, Paper 749026 ASME, 1974.

17. L. Y. Bronicki, "The Ormat Rankine Power Unit", 7th Conference Proc. IECEC, 327-334, Paper 729057, ASME 1972.

18. V. N. Moskvicheva and A. E. Popov, "Geothermal Power Plant on the Paratunka River", Geothermics, Special Issue 2, 1567-1571, 1970.

19. E. A. Farber and F. L. Prescott, "A Solar Powered V-2 Vapor Engine", presented at ISES Meeting, Paris, July 1973.

20. A. F. Clay, J. A. Day, W. C. Dickinson and L. F. Wouters, "The Shallow Solar Pond Energy Conversion System: An Analysis of a Conceptual 10 MWc Plant", Lawrence Livermore Laboratory, Report UCRL-51533, Rev. 1, 1974.

21. M. J. Shoemaker, "Notes on a Solar Collector with Unique Air Permeable Media", Solar Energy, 5, 138-41, 1961.

CAPTIONS

Fig. 1. a) Plot of collector efficiency F_c versus difference between water outlet temperature and ambient for a PPG prototype Baseline Solar Collector [2]. Insolation is 300 BTU/hr ft^2 (approximately 950 KWm^{-2}), ambient air temperature 70°F (21.1°C). Two 1/8" glass windows and 3" insulation at the back are used.

b) Plot of F_c versus ratio of temperature difference (between inlet fluid and ambient) to insolation, for a collector fabricated at NASA Lewis Research Center [1], and Solapak collector (Beasley Industries, South Australia). Ambient temperature 75°F (23.9°C), flow rate 1/3 gpm.

Fig. 2. Energy band edges and Fermi level versus distance from surface of semiconductor. Light photons penetrate about 25 microns in silicon and cause electron excitation from valence to conduction band by amount depending on photon energy (greater than band gap). The negatively charged electrons and positive "holes" are swept in opposite directions by the electric field before internal recombination can occur.

Fig. 3. Product $\eta_o = F_c \eta_c$ where F_c is taken from Fig. 1(a) and η_c is Carnot efficiency $(1 - T_1/T_2)$, plotted versus temperature difference (collector outlet minus ambient).

Fig. 4. Plots on pressure volume and temperature entropy planes, of 4 engine cycles (ideal, air standard). In all cases a-b is isentropic compression and c-d is isentropic expansion, effectively adiabatic. For the 4 cycles, b-c is (A) isothermal expansion, (B) constant volume heat addition, and (C,D) constant

pressure heat addition. The portion d-a is (A) isothermal compression (B,C) constant volume heat rejection and (D) constant pressure heat rejection. In an open cycle in (B,C,D), the air is released at d, and a new cycle effectively commences at a, with a new charge of ambient temperature air.

Fig. 5. Pressure versus volume in a Lenoir cycle, plotted numerically for the temperatures, pressures and compression shown. If the expansion is staggered using a reciprocating piston engine and the exhaust vented to the atmosphere, the equivalent cycle is as shown on the RHS.

Fig. 6. Plot of closed Lenoir cycle (section A is equivalent to open cycle) efficiency versus ratio of upper to lower temperature. The subscripts A and B refer to the work areas labeled as such in Fig. 5. The Carnot efficiency divided by 6, is also shown.

Fig. 7. Plot of T_3 in an Otto cycle (see insert) versus inverse compression ratio.

Fig. 8. Diagram of construction of low cost high pressure solar collector. Heat exchanger in this case was blackened lathe turnings for heating air.

Fig. 9. Photograph of compressor-engine assembly. Aluminum sliding cylinders close and open exhaust valves, just visible as slots to the left of aluminum. Valve lever L is actuated by pushrod with teflon bearing B fitting over piston rod. Crankshaft, flywheel and pulley are visible on right. Small unti between the brass cylinders near left side is engine/compressor valve reversal lever, actuated by a nylon thread (not visible) attached to pulley rope.

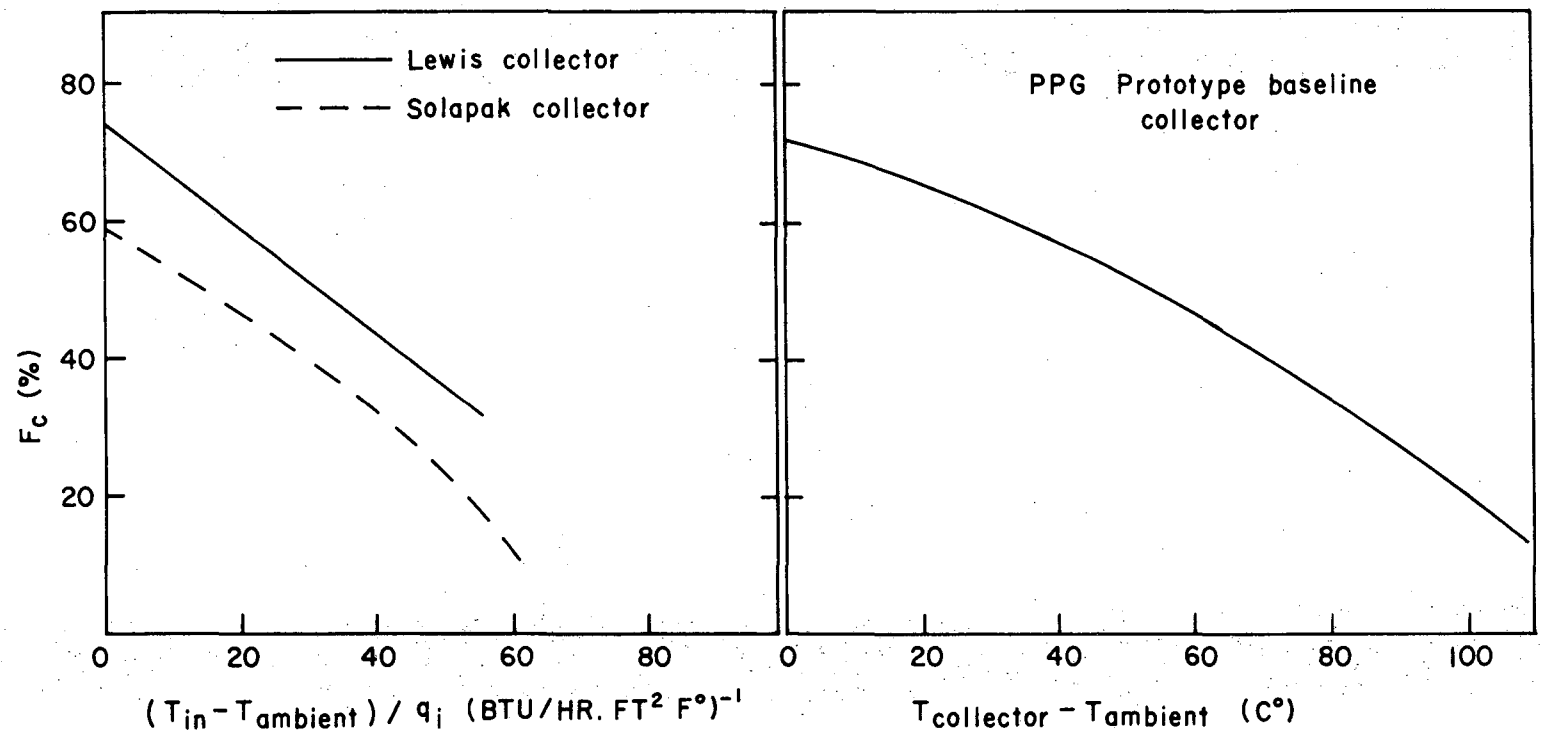

XBL752-5065

Fig. 1

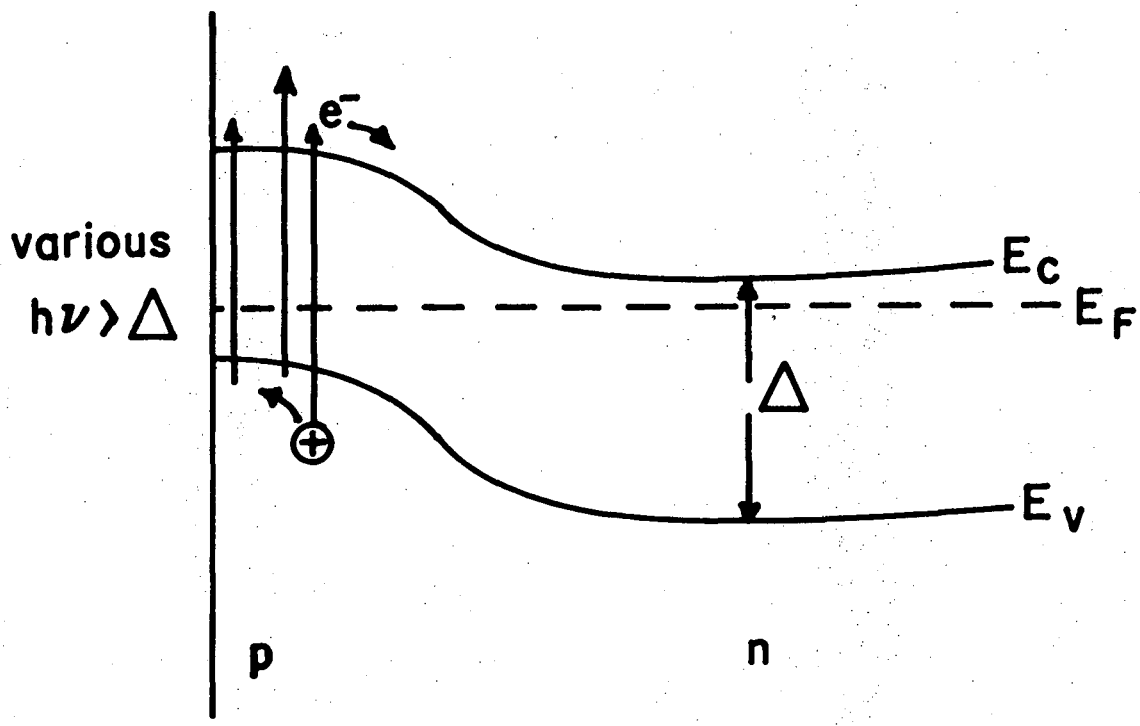

XBL752-5063

Fig. 2

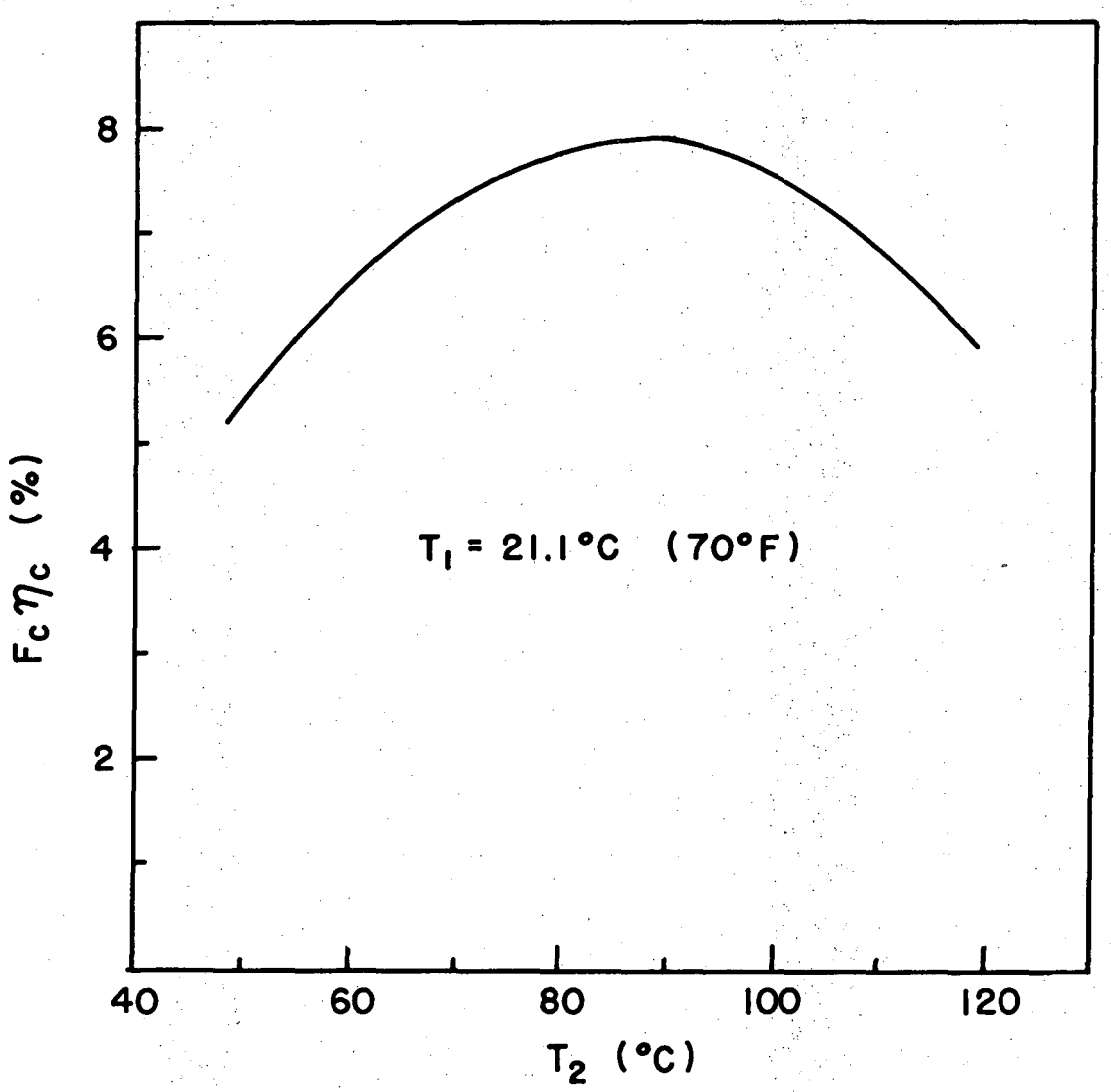

XBL752-5064

Fig. 3

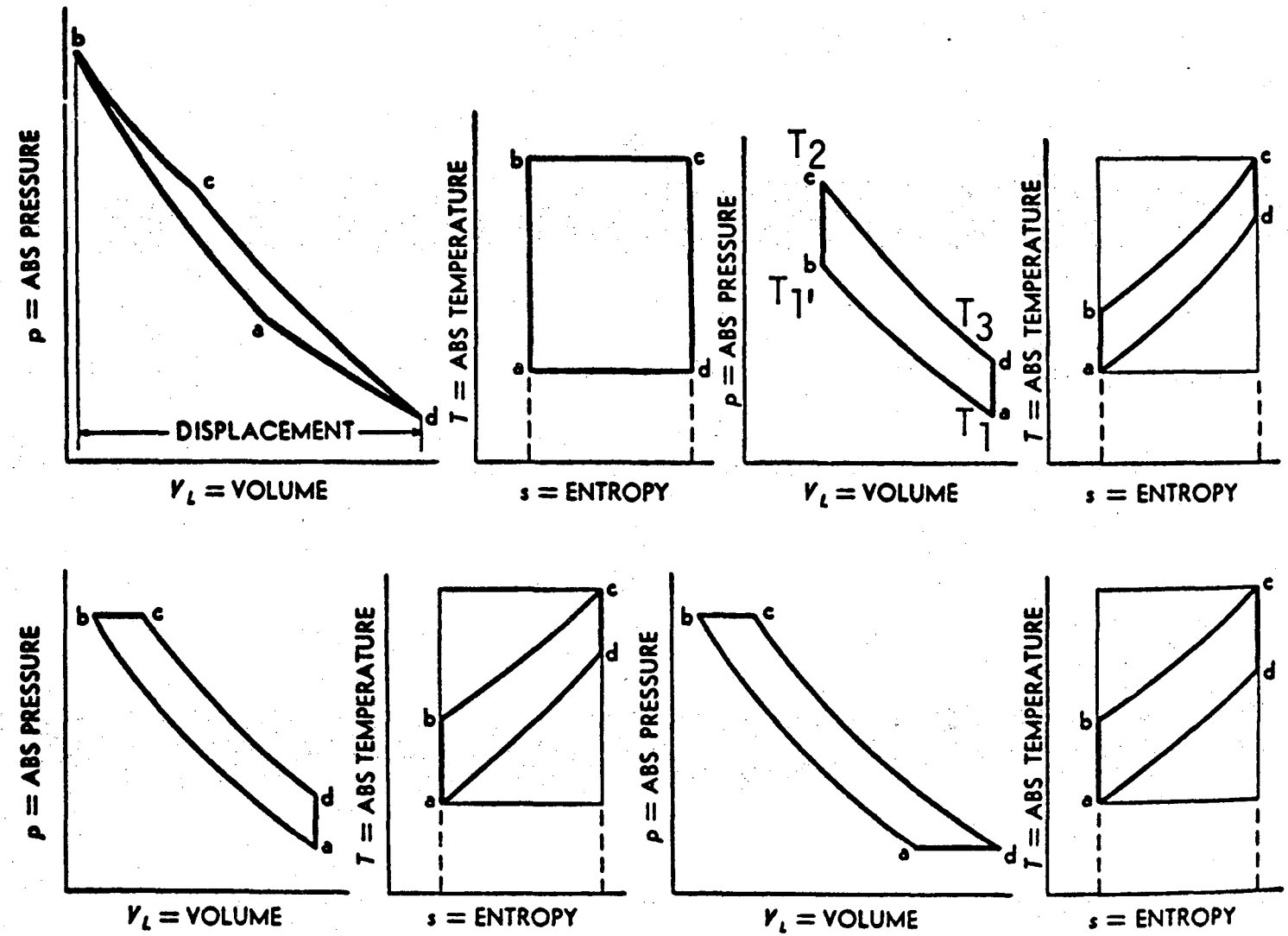

HANEMAN

Figure 4

0 0 1 4 3 0 1 4 9 0

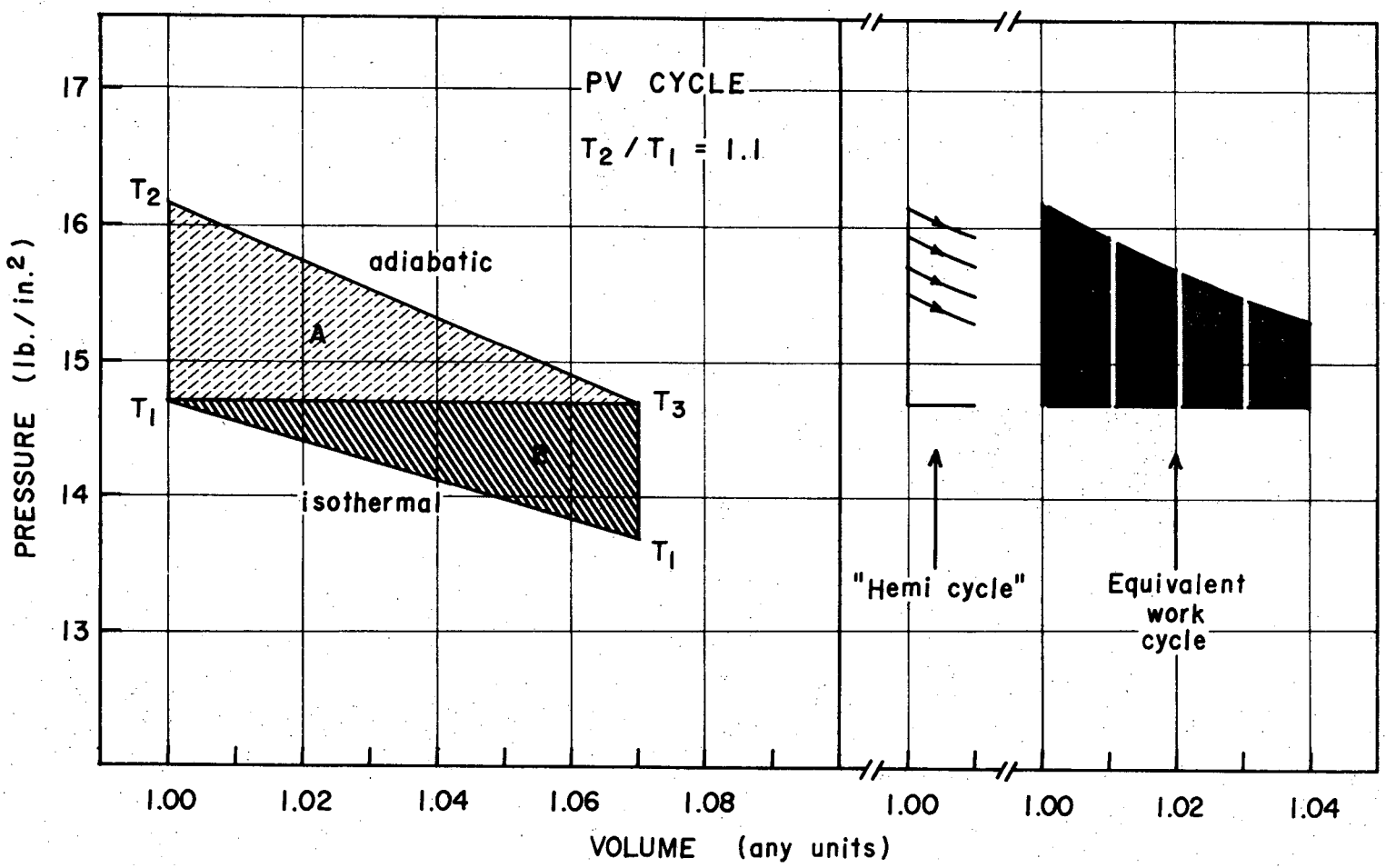

XBL748-5283

Fig. 5

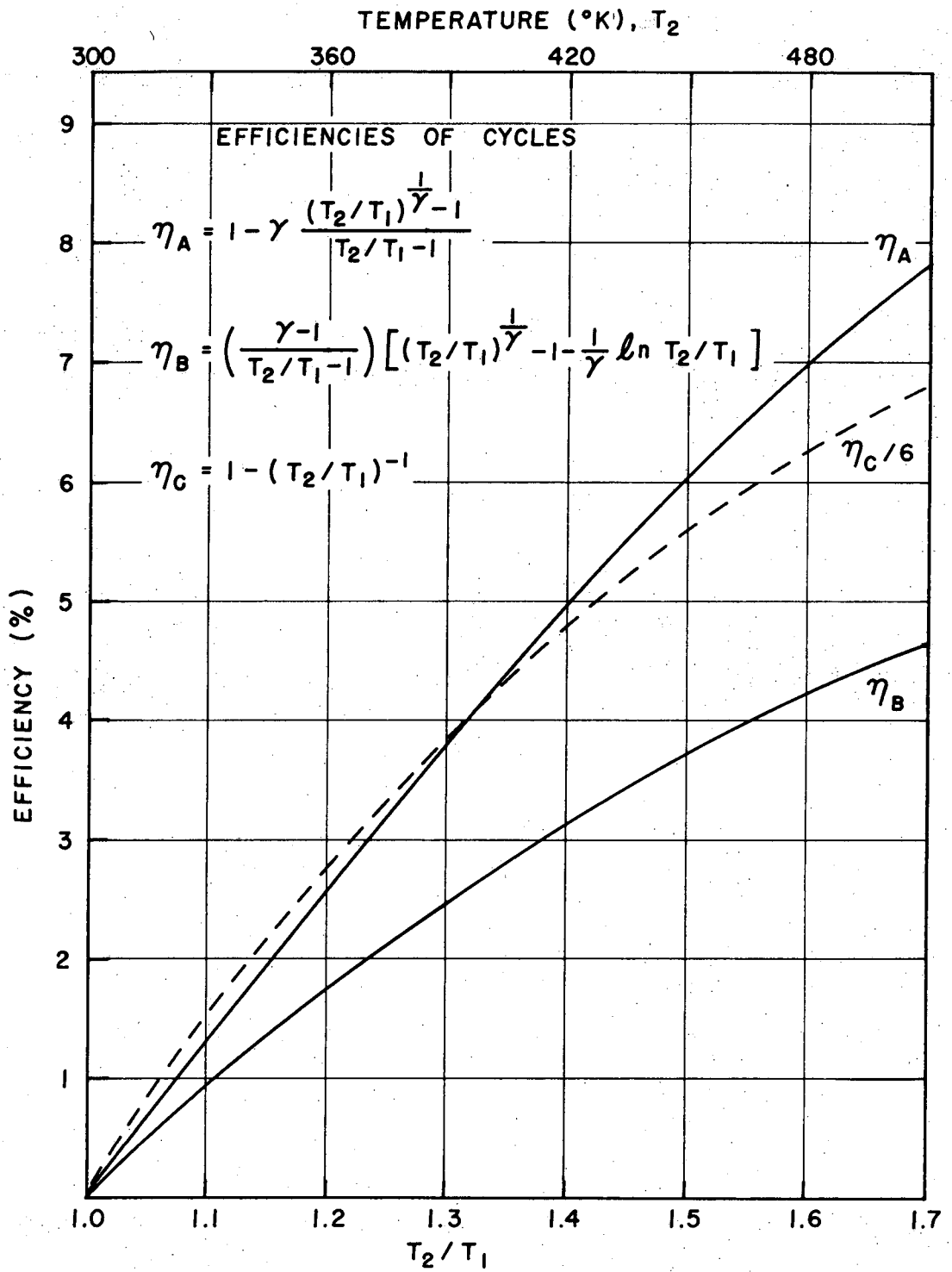

XBL748-5284

Fig. 6

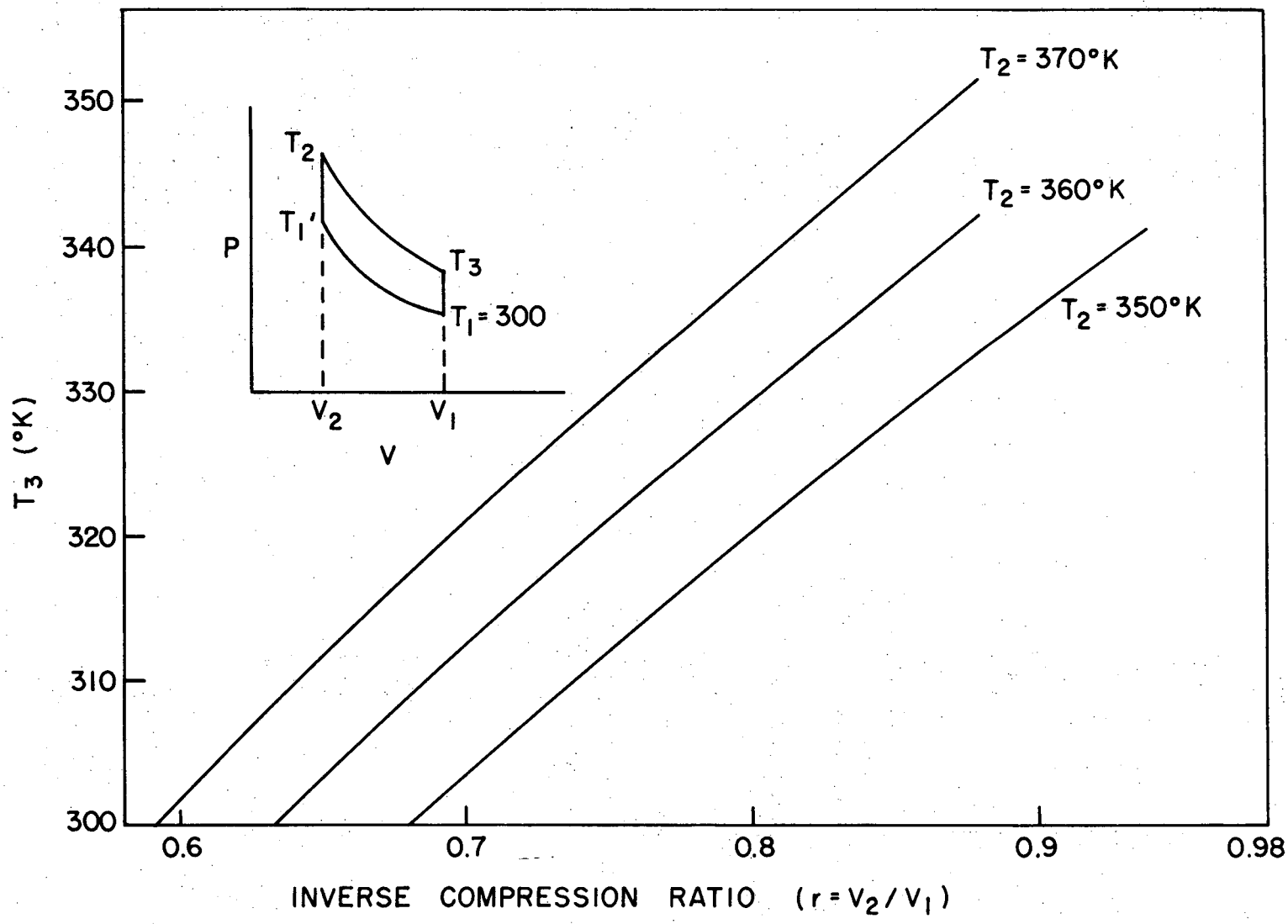

XBL752-5067

Fig. 7

0 0 0 0 4 3 0 1 4 9 2

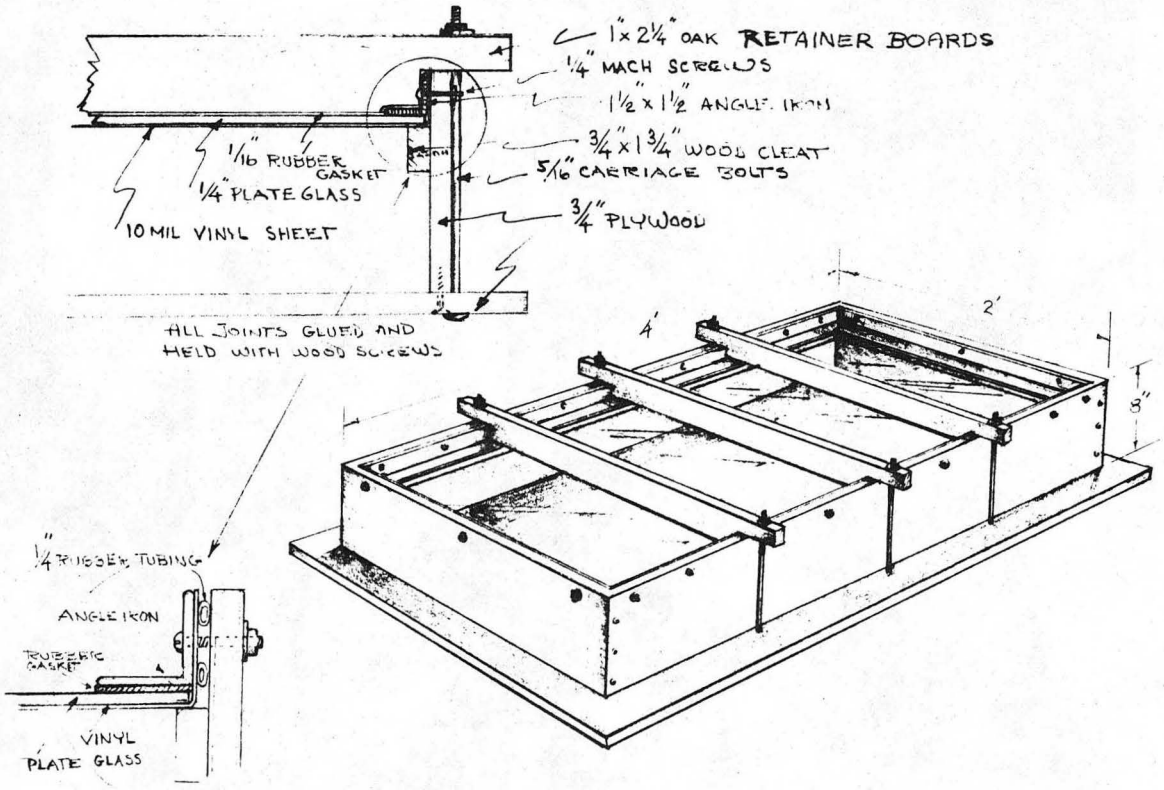

XBL 752-5066

Fig. 8

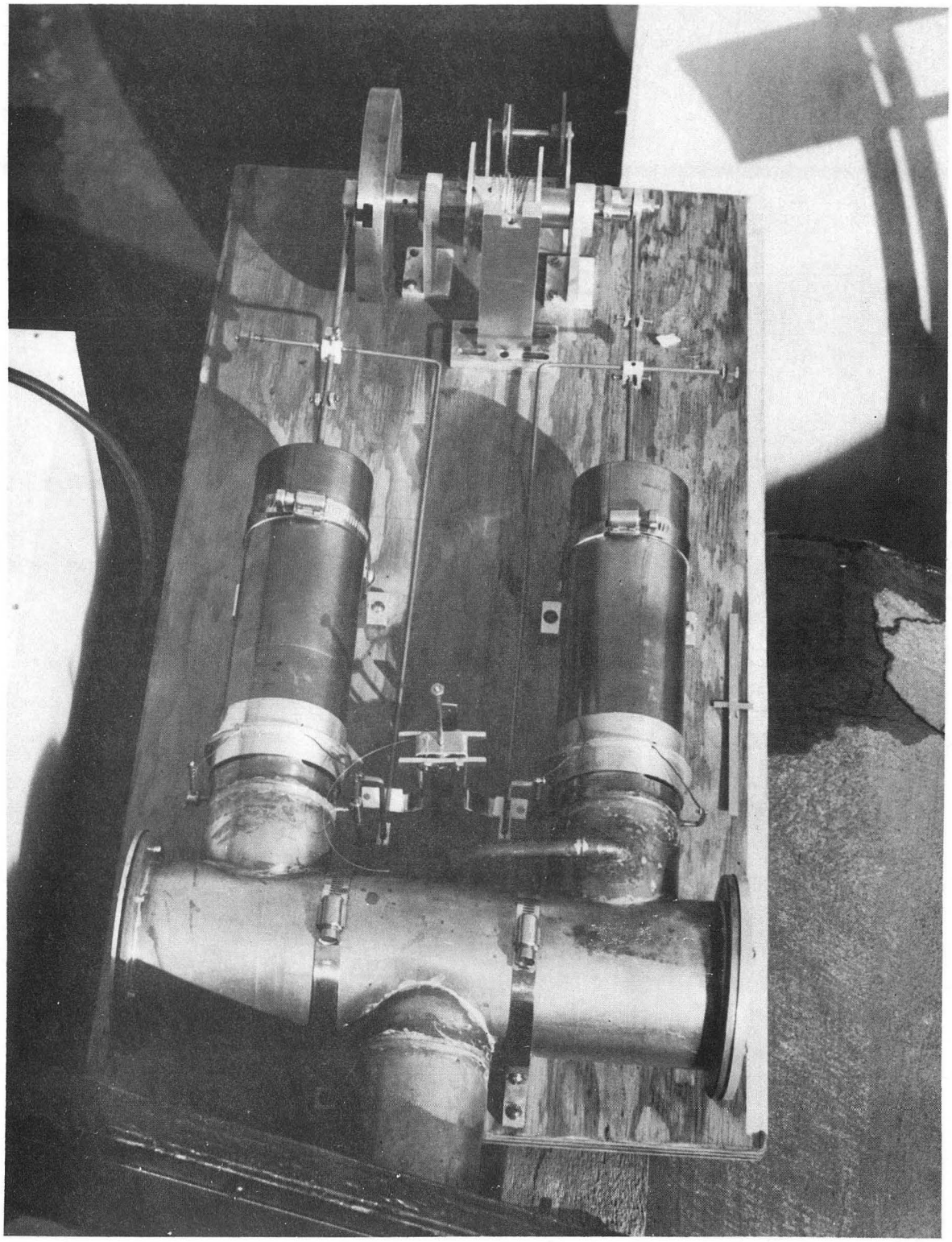

CBB 752-1083

Fig. 9

0 0 0 4 3 0 1 4 9 3

LEGAL NOTICE

This report was prepared as an account of work sponsored by the United States Government. Neither the United States nor the United States Atomic Energy Commission, nor any of their employees, nor any of their contractors, subcontractors, or their employees, makes any warranty, express or implied, or assumes any legal liability or responsibility for the accuracy, completeness or usefulness of any information, apparatus, product or process disclosed, or represents that its use would not infringe privately owned rights.

TECHNICAL INFORMATION DIVISION
LAWRENCE BERKELEY LABORATORY
UNIVERSITY OF CALIFORNIA
BERKELEY, CALIFORNIA 94720

DISCLAIMER

This document was prepared as an account of work sponsored by the United States Government. While this document is believed to contain correct information, neither the United States Government nor any agency thereof, nor the Regents of the University of California, nor any of their employees, makes any warranty, express or implied, or assumes any legal responsibility for the accuracy, completeness, or usefulness of any information, apparatus, product, or process disclosed, or represents that its use would not infringe privately owned rights. Reference herein to any specific commercial product, process, or service by its trade name, trademark, manufacturer, or otherwise, does not necessarily constitute or imply its endorsement, recommendation, or favoring by the United States Government or any agency thereof, or the Regents of the University of California. The views and opinions of authors expressed herein do not necessarily state or reflect those of the United States Government or any agency thereof or the Regents of the University of California.

0 0 0 4 3 0 1 4 9 5

REGULATION OF GLUCOSE-6-PHOSPHATE DEHYDROGENASE IN SPINACH CHLOROPLASTS BY RIBULOSE-1,5-DIPHOSPHATE AND NADPH/NADP$^+$ RATIOS*

KLAUS LENDZIAN** AND JAMES A. BASSHAM

Laboratory of Chemical Biodynamics, Lawrence Berkeley Laboratory

University of California, Berkeley, California 94720

SUMMARY

The activity of glucose-6-phosphate dehydrogenase (E.C. 1.1.1.49) from spinach chloroplasts is strongly regulated by the ratio of NADPH/NADP$^+$, with the extent of this regulation controlled by the concentration of ribulose-1,5-diphosphate. Other metabolites of the reductive pentose phosphate cycle are far less effective in mediating the regulation of the enzyme activity by NADPH/NADP$^+$ ratio. With a ratio of NADPH/NADP$^+$ of 2, and a concentration of ribulose-1,5-diphosphate of 0.6 mM, the activity of the enzyme is completely inhibited.

This level of ribulose-1,5-diphosphate is well within the concentration range which has been reported for unicellular green algae photosynthesizing *in vivo*. Ratios of NADPH/NADP$^+$ of 2.0 have been measured for isolated spinach chloroplasts in the light and under physiological conditions.

Since ribulose-1,5-diphosphate is a metabolite unique to the reductive pentose phosphate cycle and inhibits glucose-6-phosphate dehydrogenase in the presence of NADPH/NADP$^+$ ratios found in cloroplasts in the light, it is proposed that regulation of the oxidative pentose phosphate cycle is accomplished *in vivo* by the levels of ribulose-1,5-diphosphate, NADPH, and NADP$^+$.

It already has been shown that several key reactions of the reductive pentose phosphate cycle in chloroplasts are regulated by levels of $NADPH/NADP^+$ or other electron-carrying cofactors, and at least one key regulated step, the carboxylation reaction is strongly affected by 6-phosphogluconate, the metabolite unique to the oxidative pentose phosphate cycle. Thus there is an interesting inverse regulation system in chloroplasts, in which reduced/oxidized coenzymes provide a general regulatory mechanism. The reductive cycle is activated at high $NADPH/NADP^+$ ratios where the oxidative cycle is inhibited, and ribulose-1,5-diphosphate and 6-phosphogluconate provide further control of the cycles, each regulating the cycle in which it is not a metabolite.

---

* Reprint requests should be addressed to the second author.

** Present address: Institut Für Botanik, Technische Universität, 8 München 2, Arcisstr. 21, W.-Germany.

Abbreviations: RPP, reductive pentose phosphate; OPP, oxidative pentose phosphate; PMS, phenazine methosulfate; Ribul-1,5-P_2, ribulose-1,5-diphosphate; Ribul-5-P, ribulose-5-phosphate; Rib-5-P, ribose-5-phosphate; Fru-6-P, fructose-6-phosphate; Fru-1,6-P_2, fructose-1,6-diphosphate.

INTRODUCTION

Within chloroplasts of green plant cells, the reductive pentose phosphate cycle (RPP cycle, Calvin cycle) [1] operates during photosynthesis in the light, whereas the oxidative pentose phosphate cycle (OPP cycle, hexose monophosphate shunt) operates under conditions of cell respiration such as in the dark [2,3,4,5]. Although the RPP cycle is driven by ATP and NADPH formed by light reactions in the pigmented

chloroplast membranes, and the OPP cycle generates NADPH by the oxidative metabolism of carbohydrate reserves, mass action by the levels of these cofactors would be an insufficient regulatory mechanism for controlling these two cycles and preventing wasteful reactions. In particular, the free energy change accompanying the oxidation of glucose-6-phosphate to 6-phosphogluconate with the concurrent reduction of $NADP^+$ to NADPH is from -8 Kcal to -12 Kcal, depending on metabolite concentrations [6]. This reaction, mediated by glucose-6-phosphate dehydrogenase is clearly rate-limiting, even during operation of the OPP cycle. No conceivable physiological levels of the reactants and products could control it through mass action [6].

Kinetic tracer studies with unicellular algae demonstrated the immediate appearance of 6-phosphogluconate when the light was turned off [7] or in the light following addition of Vitamin K_5 [2,7]. The primary effect of Vitamin K_5 addition to the algae is thought to be the diversion of electrons coming from the light reactions, resulting in a decreased ratio of $NADPH/NADP^+$, similar to that which occurs when the light is turned off. The appearance of 6-phosphogluconate, which occurs also in isolated spinach chloroplasts upon addition of vitamin K_5, is considered to be an indication of operation of the OPP cycle [2,7].

Other results of kinetic tracer studies with algae and either light-dark changes or Vitamin K_5 addition suggested that activation of glucose-6-phosphate dehydrogenase and of the OPP cycle was accompanied by decreased activities of key regulated steps of the RPP cycle including the conversion of ribulose-5-phosphate to ribulose-1,5-diphosphate, mediated by phosphoribulokinase (E.C.2.7.1.19), the carboxylation reaction mediated by ribulose diphosphate carboxylase (E.C.4.1.1.39), and the conversions of

fructose-1,6-diphosphate and sedoheptulose-1,7-diphosphate to fructose-6-phosphate and sedoheptulose-7-phosphate respectively, mediated by hexose diphosphatase (E.C.3.1.3.11) [2]. Each of these reactions is unique to the RPP cycle, and each is characterized by a large negative free energy change under steady-state conditions in the light [6]. Thus there is an inverse relationship between the rate-limiting step of the OPP cycle (activated at low $NADPH/NADP^+$ ratios) and the rate-limiting steps of the RPP cycle (activated at high $NADPH/NADP^+$ ratios).

Besides these in vivo studies, some investigations of enzymatic activities suggested that $NADPH/NADP^+$ ratios could provide a general regulatory control in chloroplasts. Under certain conditions ribulose diphosphate carboxylase is activated by NADPH [8], while the activity of glucose-6-phosphate dehydrogenase is stimulated by $NADP^+$ [9]. In the case of the ribulose diphosphate carboxylase, however, enzyme activity was also strongly affected by physiological levels of 6-phosphogluconate. Thus, the metabolite unique to the OPP cycle was affecting a reaction unique to the RPP cycle. This led us to consider whether a metabolite unique to the RPP cycle might affect the activity of an enzyme unique to the OPP cycle.

Furthermore, with either darkness or Vitamin K_5 addition, the one metabolite of the RPP cycle which drops to a very low concentration compared with its concentration in the light is ribulose-1,5-diphosphate, the carboxylation substrate. This suggested the possibility that the high level of ribulose-1,5-diphosphate in the light might act to suppress the activity of glucose-6-phosphate dehydrogenase. Finally, Pelroy, et al. [10] found the glucose-6-phosphate dehydrogenase activity of several strains of blue-green algae to be inhibited by physiological levels of

ribulose-1,5-diphosphate. In this report we describe the effect of ribulose-1,5-diphosphate in amplifying the regulatory effects of $NADPH/NADP^+$ ratios on glucose-6-phosphate dehydrogenase activity, and as a function of pH.

MATERIALS AND METHODS

Young spinach leaves of approximately the same age were harvested from outdoor-grown plants after a 16-hour dark period. Chloroplasts were isolated according to the method of Jensen and Bassham [11]. The resulting chloroplast suspension in solution B contained about 2mg chlorophyll/ml. For comparative studies whole chloroplasts from the same batch of leaves were isolated and the soluble chloroplast protein solution was separated from the chloroplast lamellae using the method described by Bassham et al. [12], except that the chloroplasts from one batch were disrupted in 1 ml of solution Z [12]. The isolated chloroplasts and the soluble protein fraction were always kept in the dark at 2°C and were used immediately for the glucose-6-phosphate dehydrogenase assay.

Glucose-6-phosphate dehydrogenase standard assay mixtures contained 36 mM triethanolamine/HCl buffer (pH 7.6), 10 mM $MgCl_2$, 0.6 mM $NADP^+$, 1.0 mM glucose-6-phosphate and 0.1 ml of the chloroplast suspension or 0.2 ml of the solution of chloroplast soluble proteins in a final volume of 2.1 ml. The concentrations of different metabolites of the RPP cycle and of NADPH added to the assay mixture are indicated in the legends. The enzyme assays were carried out under a nitrogen atmosphere and all solutions were flushed with nitrogen before use. The chloroplasts were osmotically destroyed upon being pipetted into the hypotonic assay

solution, thus releasing the glucose-6-phosphate dehydrogenase and other soluble enzymes into the test medium. The reduction of $NADP^+$ was measured spectrophotometrically at 340 nm in quartz cuvettes of 1 cm light path using a Cary 11B spectrophotometer. Assays were performed at 20°C. The reactions were started by addition of the substrate. No detectable increase in absorbance was observed when substrate or $NADP^+$ was omitted. References always were run without substrate. Enzyme activity is expressed as amount of $NADP^+$ reduced per minute and per milligram chlorophyll and is calculated from the initial reaction velocity.

As both glucose-6-phosphate dehydrogenase and 6-phosphogluconate dehydrogenase (E.C.1.1.1.43) are present in spinach chloroplasts [13], three assays were performed to show that the presence of 6-phosphogluconate dehydrogenase does not interfere with assaying glucose-6-phosphate dehydrogenase. One assay contained 1.0 mM glucose-6-phosphate and 1.0 mM 6-phosphogluconate, the other two contained all ingredients plus glucose-6-phosphate or 6-phosphogluconate, respectively.

The sum of the initial reaction velocities of both enzymes determined in separate assays was equal to the total initial reaction velocity when both enzymes were assayed simultaneously in the same reaction mixture. Thus under the conditions described above, the presence of 6-phosphogluconate dehydrogenase did not interfere with the measurement of glucose-6-phosphate dehydrogenase activity.

Assay mixtures for the measurement of 6-phosphogluconate dehydrogenase were the same as for glucose-6-phosphate dehydrogenase except 1.0 mM 6-phosphogluconate was substituted for glucose-6-phosphate. Chlorophyll was determined according to Vernon [14].

For the determination of $NADP^+$ and NADPH levels in chloroplasts in the dark and during CO_2 fixation in the light whole choloroplasts were

isolated and were allowed to photosynthesize according to the procedure described by Jensen and Bassham [11]. A fluorometric method for measuring pyridine nucleotide levels in animal tissues described by Cartier [15] has been modified to detect very small amounts of pyridine nucleotides in chloroplasts while using a simple and rapid method for preparing samples from a kinetic experiment with photosynthesizing chloroplasts.

The following procedure was used: 0.02 ml samples were removed from a chloroplast suspension capable of fixing CO_2 in the light and were immediately injected into either 0.05 ml 0.1 N NaOH (to destroy the oxidized pyridine nucleotides and keep the reduced ones) or 0.05 ml 0.1 N HCl (to destroy the reduced pyridine nucleotides and keep the oxidized ones). The resulting samples were then immediately heated at 60°C for 20 min. Within that time the reduced pyridine nucleotides in the acid and the oxidized ones in the base are completely destroyed. After heating, the samples were kept at 0°C. Chloroplast debris were spun down at 12,000 x g for 10 min. The supernatant was used directly for the determination of $NADP^+$ and NADPH. Controls containing internal pyridine nucleotide standards were used for a standard calibration curve.

For the determination of $NADP^+$ and NADPH the following reaction sequence (continuous cycling) was used:

$$\text{Glucose-6-phosphate} + NADP^+ \xrightarrow[\text{dehydrogenase}]{\text{glucose-6-phosphate}} \text{6-phosphogluconate} + NADPH$$

$$NADPH + PMS_{oxyd.} \longrightarrow NADP^+ + PMS_{red.}$$

$$PMS_{red.} + \text{resazurine} \longrightarrow PMS_{oxyd.} + \text{resorufine}$$

The electrons from NADPH are transferred to resazurine, which is reduced to the highly fluorescent resorufine. In this redox chain the amount of resorufine is directly proportional to the amount of $NADP^+$ or NADPH if these coenzymes are present in concentrations lower than the K_m. The assay contained the following components in a final volume of 0.905 ml:

triethanolamine/HCl, pH 7.8, 77 mM (0.7 ml);

$MgCl_2$, 2.2 mM (0.02 ml);

glucose-6-P, 2.2 mM (0.05 ml);

dipyridyl, 14 μM (0.02 ml);

PMS, 0.55 mM (0.05 ml);

resazurine, 10 μM (0.05 ml);

glucose-6-phosphate dehydrogenase, 15 μg dissolved in triethanolamine buffer, 50 mM, pH 7.8 (0.015 ml);

0.005-0.02 ml samples for $NADP^+$ or NADPH determination. The concentrations indicate the final concentrations in the test system.

The optimal values for both the strength of the triethanolamine buffer and the concentration of the cofactor Mg^{2+} were determined by their respective stabilizing and enhancing effects on the enzymatic reaction. The buffer in the concentration used does not quench the fluorescent dye significantly in comparison to final buffer concentrations higher than 80 mM. Moreover, the capacity of the buffer is so high that the addition of the acidic or basic samples does not shift the pH of the test system significantly. In this way it is possible to avoid a procedure in which the samples with the pyridine nucleotides must be neutralized before measuring. Such neutralization procedures are difficult and time consuming because of the small sample sizes and the necessity of avoiding any localized pH "overshoot" which could destroy the pyridine nucleotides being measured.

The reaction was started by addition of the samples containing $NADP^+$ or NADPH after the base line of the recorder was adjusted and straight. The measurements were run in a 10 x 3 mm cuvette (3 mm side turned towards the excitation beam) at 20°C with a Hitachi MPF-2A spectrofluorometer coupled with a Hitachi recorder (sensitivity range 4, 5 or 6). The excitation wavelength was 540 nm with a band width of 8 nm; the increase of fluorescence was followed at 580 nm with a band width of 8 nm. The assay permits the determination of both $NADP^+$ and NADPH. NAD^+ and NADH do not interfere with the test system because NAD^+ cannot be reduced by glucose-6-phosphate dehydrogenase. NADH is of course oxidized by PMS to NAD^+, and PMS_{red} reduces resazurine; however, this reaction is very fast and the increase of resorufine only raises the base line, which is then adjusted before the enzyme reaction with the triphosphopyridine nucleotides is started.

The chemicals were obtained from Calbiochem, Sigma and MCB (resazurine). The acid forms of ribulose-1,5-diphosphate and 6-phosphogluconate were generated from solutions of the respective barium and tri-monocyclohexylammonium salts with Dowex-50.

RESULTS

Glucose-6-phosphate dehydrogenase from whole spinach chloroplasts incubated with 1 mM Ribul-1,5-P_2 was inhibited about 60% in the presence of just saturating amounts of its substrate glucose-6-phosphate and its coenzyme $NADP^+$ (Table I). Other intermediates of the reductive pentose phosphate cycle caused less than 10% inhibition except Ribul-5-P with an inhibitory effect of 18%.

The stability of the inhibitory effect of Ribul-1,5-P_2 over a certain period of time monitored in the test cuvette at 340 nm was directly dependent on the conditions under which the assay was conducted. Since there was a Mg^{2+} concentration of 10 mM in the assay, one had to expect possible CO_2 dark fixation in the presence of CO_2 and Ribul-1,5-P_2 [16] which would reduce the actual Ribul-1,5-P_2 concentration. Under aerobic conditions the inhibition of the enzyme activity by Ribul-1,5-P_2 was indeed slowly decreasing during the assay indicating the consumption of Ribul-1,5-P_2 by the carboxylation and/or oxygenase reaction. A further addition of Ribul-1,5-P_2 to the assay mixture during the assay brought the amount of inhibition back to the original value. Under anaerobic assay conditions, achieved under a nitrogen atmosphere, the inhibition remained stable during the time the enzyme activity was monitored. Therefore all assays were conducted under a nitrogen atmosphere and with solutions previously flushed with nitrogen. The anaerobic environment had no effect on glucose-6-phosphate dehydrogenase activity.

As the whole chloroplasts were lysed in the assay mixture, releasing glucose-6-phosphate dehydrogenase and the other soluble components from the compartment within the outer chloroplast membranes, the lamellae also remained in the test solution. This fact caused the problem of inhomogenity as the lamellae slowly sank to the bottom of the cuvette changing slightly the intensity of the 340 nm light beam going through the cuvette. This disadvantage could be eliminated by either using a reference cuvette without substrate or by using a soluble chloroplast protein solution without the lamellae as the enzyme source. The effects of different metabolites of the reductive pentose phosphate cycle on glucose-6-phosphate dehydrogenase in the soluble protein solution alone are not significantly different from those obtained by lysing whole chloroplasts in the assay mixture (Table I). As we added the same amount of enzyme to both kinds

of assay, these results are not unexpected. In preliminary experiments (data not shown) we already could show that the affinity of glucose-6-phosphate dehydrogenase for substrate and coenzyme did not change due to the different way of handling the enzyme before assaying. For all further experiments we used the soluble chloroplast protein solution as a source for glucose-6-phosphate dehydrogenase.

6-phosphogluconate dehydrogenase, the second key enzyme in the OPP cycle is unaffected by Ribul-1,5-P_2 and the other metabolites tested and was therefore not the subject of further investigations.

The inhibition of glucose-6-phosphate dehydrogenase by 1 mM RuDP could be demonstrated in the presence of just saturating substrate and coenzyme concentrations. However, under physiological conditions the concentration of the coenzyme $NADP^+$ is subject to drastic changes within the chloroplasts [17]. Fig. 1 illustrates the change of enzyme activity at decreasing $NADP^+$ concentrations and increasing Ribul-1,5-P_2 levels. Both decreasing the coenzyme concentration and increasing the Ribul-1,5-P_2 concentration results in a decrease in enzyme activity. In other words the lower the coenzyme concentration the more effective is the inhibition by Ribul-1,5-P_2. At a saturating $NADP^+$ concentration of 0.6 mM the enzyme activity can be inhibited to 50% by 0.7 mM Ribul-1,5-P_2, at 0.01 mM $NADP^+$ it can be inhibited to 50% by only 0.25 mM Ribul-1,5-P_2; that is an inhibition of about 90% of the activity found at saturating $NADP^+$ concentrations and without the addition of Ribul-1,5-P_2.

In a plot of 1/v versus 1/[$NADP^+$] at different levels of Ribul-1,5-P_2 using the data from Fig. 1 it can be shown that the inhibition of chloroplast glucose-6-phosphate dehydrogenase by Ribul-1,5-P_2 gives a noncompetitive inhibition pattern in respect to the coenzyme $NADP^+$ (Fig. 2). The K_m value for the coenzyme is calculated from the figure to be 55 μM. At that

$NADP^+$ concentration (half-saturating) there is about 50% of the enzyme activity at saturating concentrations. This can be decreased to 25% by addition of 0.5 mM Ribul-1,5-P_2.

The activity of glucose-6-phosphate dehydrogenase is, however, not only determined by the actual concentration of its oxidized coenzyme $NADP^+$ but also by the concentration of the reduced one [9]. NADPH is a competitive inhibitor of the enzyme activity in respect to the oxidized $NADP^+$ (Fig. 3).

To demonstrate how $NADP^+$ and NADPH levels are changing in intact spinach chloroplasts during dark-light-dark transitions, these two coenzymes were measured in chloroplasts which were allowed to photosynthesize. The levels of $NADP^+$ and NADPH levels are subject to very fast changes after a dark-light or a light-dark transition (Fig. 4). In the light $NADP^+$ is reduced very rapidly to NADPH. After about 1 min the levels of NADPH and $NADP^+$ reach steady-state values. Upon switching off the light a rapid oxidation of NADPH takes place. The changes of the NADPH level in the chloroplasts are always just opposite to those of the $NADP^+$ level. The NADPH/$NADP^+$ ratios are about 0.2-0.5 in the dark but increase after a dark-light transition very fast up to 1.5-2.5 depending on a previous dark phase or the pattern of dark-light-dark alternation (Fig. 4).

The antagonistic effect of $NADP^+$ and NADPH on chloroplast glucose-6-phosphate dehydrogenase is demonstrated in Fig. 5, where the enzyme activity is plotted against different ratios of NADPH/$NADP^+$. At pH 7.6 and a ratio of 1 the enzyme activity is inhibited up to about 50%. A complete inhibition can be reached at a ratio of 2.4 and higher. At pH 8.2, an increasing ratio decreases the enzyme activity much faster than at pH 7.6. The inhibition is already complete at a NADPH/$NADP^+$ ratio of 1.5. Full

enzyme activity is maintained at ratios up to about 0.25 at both pH values.

In a further experiment we were interested in the change of glucose-6-phosphate dehydrogenase activity in the presence of certain $NADPH/NADP^+$ ratios and by adding increasing amounts of Ribul-1,5-P_2. For this experiment we chose ratios of 0.5, 1.0, and 2.0 at a pH value of 7.6 (Fig. 6). Under these conditions Ribul-1,5-P_2 became an even more effective inhibitor in the presence of increasing $NADPH/NADP^+$ ratios. At a ratio of 1 the enzyme activity is decreased by about 50% (cf. Fig. 5) corresponding to the same enzyme activity at a half-maximal concentration of $NADP^+$ in the absence of NADPH (cf. Fig. 1 and 2). In the latter case a concentration of 0.5 mM Ribul-1,5-P_2 was necessary for the inhibition of the enzyme activity up to 75%, while at a ratio of 1, a concentration of 0.3 mM Ribul-1,5-P_2 has already the same inhibitory effect. At high $NADPH/NADP^+$ ratios such as exist in chloroplasts in the light <u>in vivo</u> [17], the inhibitory effect of Ribul-1,5-P_2 becomes even stronger. Addition of 0.5 mM Ribul-1,5-P_2 at a ratio of 2 brings the inhibition to nearly 100%.

With an increase in pH of the assay mixture to a value of 8.2, the relative inhibition by Ribul-1,5-P_2 within a concentration range from 0.1-1.0 mM is not different from that at pH 7.6 (Fig. 7). Even with an $NADPH/NADP^+$ ratio of 0.5 there is no difference in the relative inhibition at the two pH values. However, the inhibitory effect of Ribul-1,5-P_2 increases at higher ratios. This effect is even more severe at the high pH (compare the two curves for the ratio of 1 in Fig. 6 and 7). Thus, Ribul-1,5-P_2 is a most effective inhibitor for glucose-6-phosphate dehydrogenase at high $NADPH/NADP^+$ ratios and in a slightly alkaline medium.

DISCUSSION

In an earlier study [6] standard physiological free energy changes of reactions of the reductive and oxidative pentose phosphate cycle were measured during steady-state photosynthesis in Chlorella pyrenoidosa. Using the criterion of large negative free energy changes as an indicator for reactions catalized by regulated enzymes, the oxidation of glucose-6-phosphate, mediated by glucose-6-phosphate dehydrogenase, with a free energy change of -8.4 kcal was already considered a regulated step in the oxidative pentose phosphate cycle in chloroplasts. Direct measurements of the enzyme activity in spinach chloroplasts have shown that the enzyme is activated in the dark and inhibited up to 70-80% in the light [9]. This inhibition in the light occurs within the first minute after a dark-light transition and is completed after 1-2 min illumination.

Another indication of the different activities of glucose-6-phosphate dehydrogenase in light and darkness is the immediate appearance of 6-phosphogluconate acid in the dark or with vitamin K_5 addition in a substantial amount in tracer studies with spinach chloroplasts [2] or Chlorella pyrenoidosa [7]. This intermediate was not detectable in the light, without vitamin K_5 addition. These findings led to the concept of exclusive operation of the oxidative pentose phosphate cycle in the dark and of the reductive pentose phosphate cycle in the light [7].

From results first indicated in an earlier communication [9] and further elaborated above, it is clear that the general regulation of the activity of glucose-6-phosphate dehydrogenase is determined by the ratio of the reduced to the oxidized state of its coenzyme $NADP^+$. However, the reaction in vivo, with a ΔG^s of -8 to -12 Kcal, is essentially irreversible, and the concentrations of reactants and substrates have little

or no effect on rate via mass action, since all are in the 0.01 mM to 1.0 mM range. Thus a specific regulatory effect of NADPH and $NADP^+$ on enzyme activity is required.

As the outer chloroplast membranes are impermeable towards pyridine nucleotides, the total concentration of oxidized plus reduced pyridine nucleotides is quite constant under certain physiological conditions in chloroplasts of different sources [17]. However, as the present study shows, the ratio of $NADPH/NADP^+$ in spinach chloroplasts undergoes drastic changes after dark-light or light-dark transitons. Upon illumination of whole chloroplasts a rapid reduction of $NADP^+$ to NADPH by photoelectrons occurs, increasing the $NADPH/NADP^+$ ratio. This ratio changes from about 0.1-0.3 in the dark up to 2.0-2.5 in the light and drops again to its original value after a light-dark transition. In contrast to an earlier report by Heber and Santarius [17], the present study shows that the ratios in whole chloroplasts determined during a dark or light period are quite constant over many minutes. The ratio seems to fall off slightly in a longer light period always accompanied by a slight levelling off of the CO_2 fixation rate. It appears that the maintenance of a constant fixation rate is directly correlated with at least the ability of the photoelectron flux to keep a certain concentration of $NADP^+$ in its reduced form. It can be assumed that the $NADPH/NADP^+$ ratio is kept quite constant <u>in vivo</u> maintaining the highest level of reducing power for reducing 3-phosphoglycerate and for regulating enzyme activities. The total amount of NADPH plus $NADP^+$ in whole chloroplasts illuminated or kept in the dark remains almost unchanged, indicating that in our chloroplast preparations neither a light-induced conversion of NAD^+ to $NADP^+$ reported by Oh-Hama and Miyachi [19] occurs

nor is an active phosphatase present which cleaves either $NADP^+$ or NADPH to NAD^+ or NADH [20]. As the sum of the triphosphopyridine nucleotides concentration in our measurements is constant, the occurence of both kinase and phosphatase at the same time would at least have no effect on the overall value of the $NADPH/NADP^+$ ratio and the total amount of triphosphopyridine nucleotides.

The $NADPH/NADP^+$ ratios determined in whole chloroplasts during a light or dark period can be simulated in reconstituted chloroplast preparations capable of photosynthesis [12]. In such preparations, all enzymes of the reductive and oxidative pentose phosphate cycle are present as well as the chloroplast lamellae system. To this system is added known amounts of NADPH and $NADP^+$. In this system, glucose-6-phosphate dehydrogenase activity is a direct reflection of the $NADPH/NADP^+$ ratio present in the assay mixture. In the presence of high ratios (up to 2.5) corresponding to conditions during illumination in whole chloroplasts, the enzyme activity is strongly or totally inhibited, while with low ratios between 0.1-0.5 corresponding to the redox state *in vivo* during the dark, the enzyme is active. Ratios between these two ranges are passed quickly during a light-dark transition or dark-light transition.

In whole chloroplasts, the kinetics of the changes of the $NADPH/NADP^+$ ratio after turning off the light are similar to those of the appearance of 6-phosphogluconic acid in the dark in *Chlorella* [7], indicating the operation of glucose-6-phosphate dehydrogenase. A similar correlation can be seen between the kinetics of glucose-6-phosphate dehydrogenase inhibition (as indicated by 6-phosphogluconate disappearance) and increase in the $NADPH/NADP^+$ ratio after a dark-light transition.

It was reported earlier that the inhibition of glucose-6-phosphate dehydrogenase in spinach chloroplasts is complete after 20 min illumination [9]. However with the improved technique for assaying the enzyme reported here we now see that the inhibition of the enzyme activity is complete after 1-2 min light. This time period is the same as that in which the ratio $NADPH/NADP^+$ in chloroplasts increases rapidly and reaches the level in the light and 6-phosphogluconate disappears in Chlorella in light.

In simulating the $NADPH/NADP^+$ ratio measured in whole chloroplasts, the question of the proper concentrations of NADPH and $NADP^+$ arose. As we do not know the exact volume of the chloroplast compartment, we can only roughly estimate the total triphosphopyridine nucleotides concentration to be between 0.05-1.0 mM. Since we chose concentrations in the upper part of this range and since the reported inhibition by Ribul-1,5-P_2 becomes relatively stronger with decreasing $NADP^+$ concentrations, all the described inhibitions should be even stronger at lower $NADP^+$ concentrations. For glucose-6-phosphate and the Mg^{+2} those concentrations were used which gave the maximal velocity of enzyme activity under our assay conditions. A concentration of 0.4 mM Ribul-1,5-P_2 during steady-state photosynthesis inside the chloroplasts of photosynthesizing Chlorella pyrenoidosa has been estimated, based on steady-state levels of ^{14}C found during photosynthesis with $^{14}CO_2$ [6]. Thus, a concentration in the range of 0.1-1.0 mM RuDP in spinach chloroplasts photosynthesizing in air (0.03% CO_2) may be within the normal physiological range.

Another set of compounds undergoing change in concentration between light and dark are the adenylates. It is known that ATP is involved in the regulation of glucose-6-phosphate dehydrogenase in several

organisms [21-24]. However, ATP concentration has no effect on the enzyme activity in spinach chloroplasts (Table I). Experiments with vitamin K_5 added to spinach chloroplasts demonstrated that while the oxidative pentose phosphate cycle is activated upon addition of the vitamin in the light, the ATP level is almost unaffected [2]. Different ATP concentrations in the presence of NADPH also have no inhibitory effect. Thus there is no evidence for a regulatory participation of ATP in the operation of the oxidative pentose phosphate cycle in spinach chloroplasts.

Other key steps in the reductive cycle may also be affected by the redox level of cofactors in the chloroplasts. The addition of vitamin K_5 to Chlorella, diverting electrons and inducing the operation of the OPP as revealed by immediate 6-phosphogluconate appearance, also caused a sudden rise in fructose-1,6-diphosphate and sedoheptulose-1,7-diphosphate [2]. This is indicative of an inactivation of the respective diphosphatase activities. The hydrolyses of these two sugar diphosphates to their monophosphates have been identified as key regulated steps of the RPP cycle from a variety of kinetic and enzymatic evidence [2,5,7]. Moreover, now it appears that the conversion of ribulose-5-phosphate to ribulose-1, 5-diphosphate, mediated by phosphoribulokinase, also stops rapidly in the dark, or upon diversion of electrons with vitamin K_5 [2,5]. There thus appears to be a general regulatory mechanism in chloroplasts in which the ratio of reduced to oxidized cofactors controls the activities of the principal regulated steps of the OPP and RPP cycles. While $NADPH/NADP^+$ ratio is implicated in the glucose-6-phosphate dehydrogenase and ribulose diphosphate carboxylase mediated reactions, control of phosphoribulokinase and of hexose/heptose diphosphate mediated steps may be via the reduced to oxidized ratio of some other cofactor such as ferredoxin [25,26]. It is

possible that another general regulatory factor could be the ratio of adenylates, since ATP/ADP ratio, or "energy-charge" is important in other systems. However, there is little evidence for this in spinach chloroplasts to date.

Besides the general regulatory mechanism, it is now clear that there are some specific metabolite controls. Thus Ribul-1,5-P_2 effects the glucose-6-phosphate dehydrogenase only in the light and 6-phosphogluconate effects ribulose diphosphate carboxylase only under dark conditions, since these fine regulators are only present in measurable and effecting amounts under certain physiological conditions (light or dark). Both NADPH and $NADP^+$ have the same binding site on the glucose-6-phosphate dehydrogenase molecule, competing each other for this site. Ribul-1,5-P_2 is a noncompetitive inhibitor with respect to $NADP^+$, and thus shows the characteristics of allosteric binding, effecting the coenzyme binding site in favoring the binding of NADPH in the presence of Ribul-1,5-P_2. This explains the increasing inhibition of the enzyme activity by Ribul-1,5-P_2 at increasing NADPH/$NADP^+$ ratios. It further illustrates one kind of interaction between a general regulator and a specific regulator. The specific regulator, Ribul-1,5-P_2 in this case, amplifies the already present control by NADPH/$NADP^+$ ratio.

Among the intermediates of the RPP cycle, Ribul-1,5-P_2 is the only effective inhibitor of glucose-6-phosphate dehydrogenase in spinach chloroplasts. Its inhibitory effect must play an important physiological role in the chloroplasts metabolism in respect to the regulation of the oxidative pentose phosphate cycle. The slight inhibition by ribulose-5-phosphate found in the incubation experiments with the chloroplast enzymes (Table I) is perhaps due to some endogenous phosphorylation, mediated by

phosphoribulose kinase. During a dark period the $NADPH/NADP^+$ ratio is low, and thus the rate of the oxidative pentose phosphate cycle is uninhibited. Furthermore the level of Ribul-1,5-P_2 will be very low or zero [6]. Under such conditions, the oxidation of glucose-6-phosphate proceeds at a substantial rate. The reaction still is not reversible, and remains the rate limiting step for the OPP cycle. Given the large negative free energy change for the reaction [6], the concentration of glucose-6-phosphate would drop below the limits of detection if the oxidation of glucose-6-phosphate became very rapid. This does not occur although there is a drop to about 1/2 of the light steady state value [6]. Since the binding constant of 6-phosphogluconic acid dehydrogenase is about 0.09 mM [27], the concentration of 6-phosphogluconate rises to an appreciable level: about 0.07 mM in Chlorella pyrenoidosa [6]. This explains the appearance of labelled 6-phosphogluconic acid as an indicator of the operation of the oxidative cycle [2].

At the beginning of a light period $NADP^+$ is quickly reduced and ADP is phosphorylated resulting in a high $NADPH/NADP^+$ and ATP/ADP ratio. The high $NADPH/NADP^+$ ratio slows the activity of glucose-6-phosphate dehydrogenase immediately. Simultaneously the 6-phosphogluconate level decreases rapidly and can't further serve as an activator of ribulose diphosphate carboxylase but is replaced by NADPH as an activator [28]. The increased level of reduced cofactors apparently activates phosphoribulokinase, and with ATP produced by light reactions, ribulose-5-phosphate is converted to ribulose-1,5-diphosphate. This substrate for the carboxylation reaction also serves to inhibit further the oxidation of glucose-6-phosphate (Fig. 5-7). Moreover, the pH in the stroma increases in the light [29] due to proton pumping into the thylakoids [30]. This higher pH amplifies the inhibitory

effect of Ribul-1,5-P_2 and the high $NADPH/NADP^+$ ratio. In this way the OPP cycle is turned off and the RPP cycle is turned on without the occurence of wasteful reactions.

ACKNOWLEDGEMENT

The investigations described in this paper were sponsored, in part, by the U.S. Atomic Energy Commission. One of the authors (K. L.) is a Deutsche Forschungsgemeinschaft fellow, 1973-75.

TABLE I

THE EFFECT OF DIFFERENT METABOLITES OF THE RPP CYCLE AND ATP ON THE ACTIVITY OF GLUCOSE-6-PHOSPHATE DEHYDROGENASE

The assay mixture contained 10 mM $MgCl_2$, 0.6 mM $NADP^+$, 1 mM glucose-6-phosphate and 0.1 ml or 0.2 ml chloroplast suspension or chloroplast soluble protein solution, respectively, in 36 mM triethanolamine/HCl buffer. The compounds were added with the enzyme. After mixing all ingredients the reaction was started after 1 minute. The control corresponds to an enzyme activity of 0.045 moles $NADP^+$ reduced x mg^{-1} chlorophyll x min^{-1} (= 100%) in both assays with whole chloroplasts or protein solution of the reconstituted system. The data results from at least four independent experiments.

Compound		% of Control (whole chloroplasts)	% of Control (Protein solution of reconstituted system)
control		100	100
Fru-1,6-P_2	1mM	91	92
Fru-6-P	1mM	103	99
PGA	1mM	94	95
Ru-5-P	1mM	97	95
Ribul-5-P	1mM	82	84
Ribul-1,5-P_2	1mM	38	40
ATP	1mM	96	99

REFERENCES

1 Bassham, J. A., Benson, A. A., Kay, L. D., Harris, A. Z., Wilson, A. T., and Calvin, M. (1954) J. Am. Chem. Soc. 76, 1760-1770

2 Bassham, J. A., and Krause, G. H. (1969) Biochim. Biophys. Acta 172, 553-565

3 Lendzian, K., and Ziegler, H. (1970) Planta 94, 27-36

4 Bassham, J. A. (1971) Science 172, 526-534

5 Bassham, J. A. (1971) Proc. 2nd International Congress on Photosynthesis Research, Stresa, ed. by G. Forti, M. Avron and A. Melandri, pp. 1723-1735, Dr. W. Junk N.V., The Hague

6 Bassham, J. A., and Krause, G. H. (1969) Biochim. Biophys. Acta 189, 207-221

7 Bassham, J. A., and Kirk, M. (1968) in "Comparative Biochemistry and Biophysics of Photosynthesis", K. Shibata, A. Takamiya, A. T. Jagendorf, and R. C. Fuller, eds., University of Tokyo Press, pp. 365-378

8 Chu, D. K., and Bassham, J. A. (1973) Plant Physiol. 52, 373-379

9 Lendzian, K., and Ziegler, H. (1972) in 2nd International Congress Photosynthesis Research 1971 (G. Forti, M. Avron and A. Melandri, eds.) Vol. III, pp. 1831-1838, Junk, Publisher, The Hague

10 Pelroy, R. A., Rippka, R., and Stanier, R. Y. (1972) Arch. Microbiol. 87, 303-322

11 Jensen, R. G., and Bassham, J. A. (1966) Proc. Natl. Acad. Sci. (U.S.) 56, 1095-1101

12 Bassham, J. A., Levine, G. A., and Forger, J. (1974) Plant Sci. Letters 2, 15-21

13 Heber, U., Hallier, U. W., and Hudson, M. A. (1967) Z. Naturforsch. 22b, 1200-1215

14 Vernon, L. P. (1960) Anal. Chem. 32, 1144

15 Cartier, P. H. (1968) Eur. J. Biochem. 4, 247-255

16 Jensen, R. G. (1971) Biochim. Biophys. Acta 234, 360-370

17 Heber, U. and Santarius, K. A. (1965) Biochim. Biophys. Acta 109, 390-408

18 Lowry, O. H., Passonneau, J. V., and Rock, M. K. (1961) J. Biol. Chem. 236, 2756-2759

19 Oh-Hama, T., and Miyachi, S. (1959) Biochim. Biophys. Acta 34, 202

20 Forti, G., Tognoli, C., and Parisi, B. (1962) Biochim. Biophys. Acta 62, 251

21 Greenhouse, W. V., Nowaki, H., and Coe, E. L. (1969) Biochim. Biophys. Acta 191, 167-169

22 Smith, J. E. and Anwer, M. S. (1971) Experientia 27, 835-836

23 Blackkolb, F., and Schlegel, H. G. (1968) Arch. Mikrobiol. 63, 177-196

24 Avigad, D. (1966) Proc. Nat. Acad. Sci. U.S.A. 56, 1543-1547

25 Buchanan, B. B., Schürmann, P., and Kalberer, P. P. (1971) J. Biol. Chem. 246, 5952-5959

26 Schürmann, P., and Buchanan, B. B. (1975) Biochim. Biophys. Acta, in press

27 Lendzian, K. (1973) in Effect of Light on Glucose-6-phosphate Dehydrogenase in Spinach Chloroplasts, Ph.D. Thesis, Technical University of Munich, W.-Germany

28 Chu, D. K., and Bassham, J. A. (1974) Plant Physiol. 54, 556-559

29 Heldt, H. W., Werdan, K., Milovancev, M., and Geller, G. (1973) Biochim. Biophys. Acta 314, 224-241

30 Neumann, G. and Jagendorf, A. T., (1964) Arch. Biochem. Biophys. 107, 109-119

FIGURE CAPTIONS

Fig. 1. Inhibition of chloroplast glucose-6-phosphate dehydrogenase by Ribul-1,5-P_2 at different $NADP^+$ concentrations. Concentrations of $NADP^+$ are indicated in the figure. Coenzyme and inhibitor were added to the assay mixture before 0.2 ml of soluble protein solution was added. The controls without Ribul-1,5-P_2 corresponds to enzyme activities of 0.043, 0.026, 0.020 and 0.010 μmoles $NADP^+$ reduced x mg^{-1} chlorophyll x min^{-1} at $NADP^+$ concentrations of 0.600, 0.090, 0.045 and 0.010 mM, respectively.

Fig. 2. Inhibition of chloroplast glucose-6-phosphate dehydrogenase by Ribul-1,5-P_2 at different $NADP^+$ concentrations. Concentrations of Ribul-1,5-P_2 are indicated in the figure. The enzyme solution was added after all ingredients except the substrate were in the assay mixture. The reaction was started by adding the substrate.

Fig. 3. Inhibition of chloroplast glucose-6-phosphate dehydrogenase by NADPH at different concentrations of $NADP^+$. Concentrations of NADPH are indicated in the figure. All other ingredients of the assay mixture are those of the standard assay mixture.

Fig. 4. Changes in the levels of $NADP^+$ and NADPH in intact spinach chloroplasts in a dark-light-dark-light transition. The dark periods are indicated by black bars. $NaHCO_3$ in a final concentration of 6 mM was added during the first light period at 5 min (indicated by arrow). The NADPH/$NADP^+$ ratios are indicated in the lower part of the graph. The fixation rate of $^{14}CO_2$ into acid-stable products was 116 μmoles x mg^{-1} chlorophyll x h^{-1}.

Fig. 5. Inhibition of chloroplast glucose-6-phosphate dehydrogenase activity at different $NADPH/NADP^+$ ratios and at two different pH values (•—• pH 7.6; o—o pH 8.2). The concentration of $NADP^+$ was kept constant at 0.6 mM, while the concentration of NADPH was changed giving the ratios indicated in the figure. The two controls without NADPH were considered as 100% and correspond to enzyme activities of 0.045 (at pH 7.6) and 0.039 (at pH 8.0) μmoles $NADP^+$ reduced x mg^{-1} chlorophyll x min^{-1}.

Fig. 6. Inhibition of chloroplast glucose-6-phosphate dehydrogenase by Ribul-1,5-P_2 at different $NADPH/NADP^+$ ratios. The concentration of $NADP^+$ was kept constant at 0.6 mM while the concentration of NADPH was changed giving the following ratios: •—• without NADPH; x—x $NADPH/NADP^+$ = 0.5; o—o $NADPH/NADP^+$ = 1.0; □—□ $NADPH/NADP^+$ = 2.0. The assays were run at pH 7.6. The controls (= 100%) without Ribul-1,5-P_2 correspond to enzyme activities of 0.046, 0.034, 0.022, and 0.006 μmoles $NADP^+$ reduced x mg^{-1} chlorophyll x min^{-1} for the ratio of 0, 0.5, 1.0, and 2.0, respectively.

Fig. 7. Inhibition of chloroplast glucose-6-phosphate dehydrogenase by Ribul-1,5-P_2 at $NADPH/NADP^+$ ratios of 0.0 (•—•); 0.5 (x—x); 1.0 (o—o). The assays were run at pH 8.2. The controls (= 100%) without Ribul-1,5-P_2 correspond to enzyme activities of 0.039, 0.024, and 0.012 μmoles $NADP^+$ reduced x mg^{-1} chlorophyll x min^{-1} for the ratios of $NADPH/NADP^+$ of 0.0, 0.5, and 1.0, respectively. The other test conditions were the same as in Fig. 5.

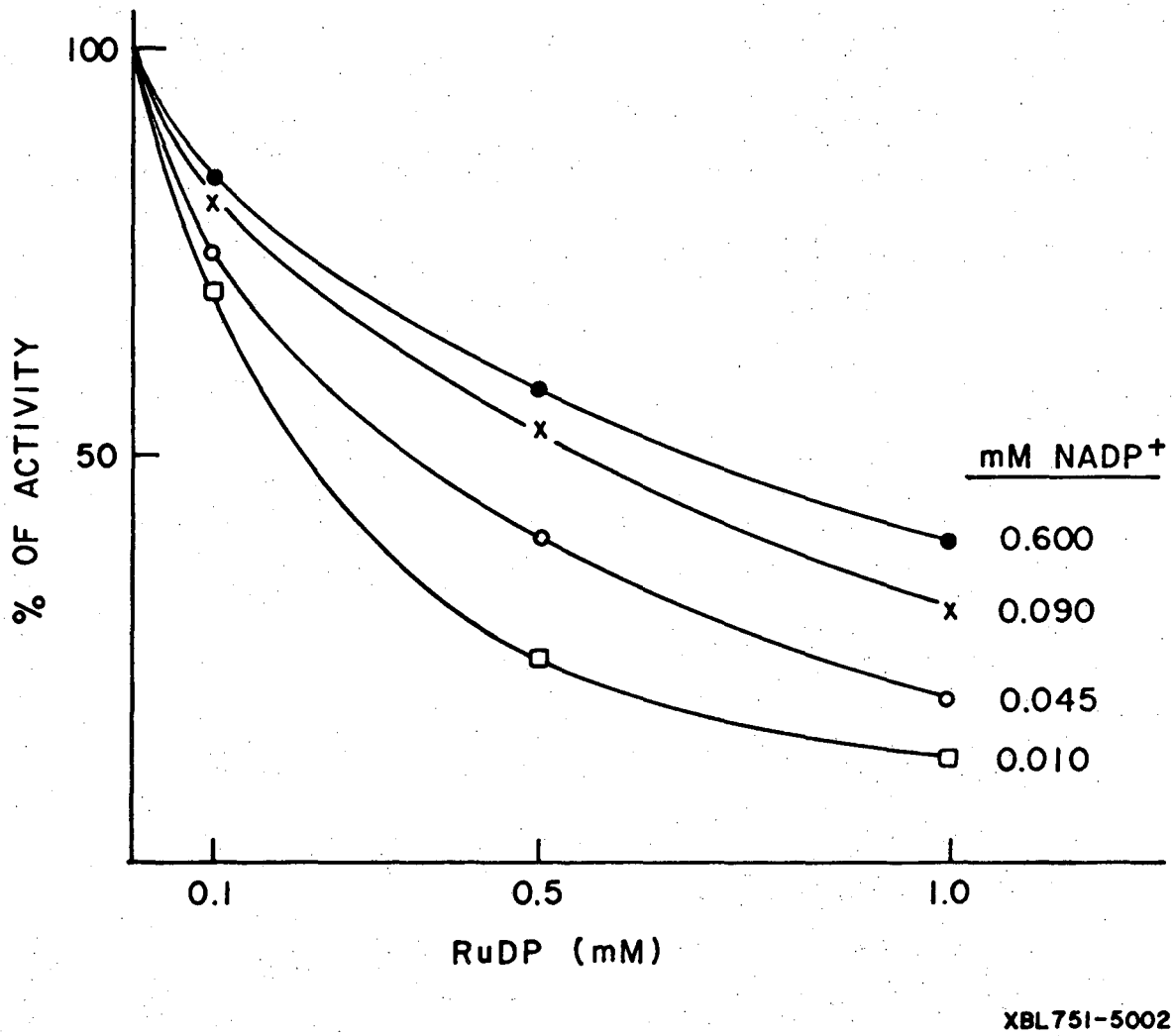
100
50
% OF ACTIVITY
mM NADP+
0.600
0.090
0.045
0.010
0.1
0.5
1.0
RuDP (mM)
XBL751-5002

Fig. 1

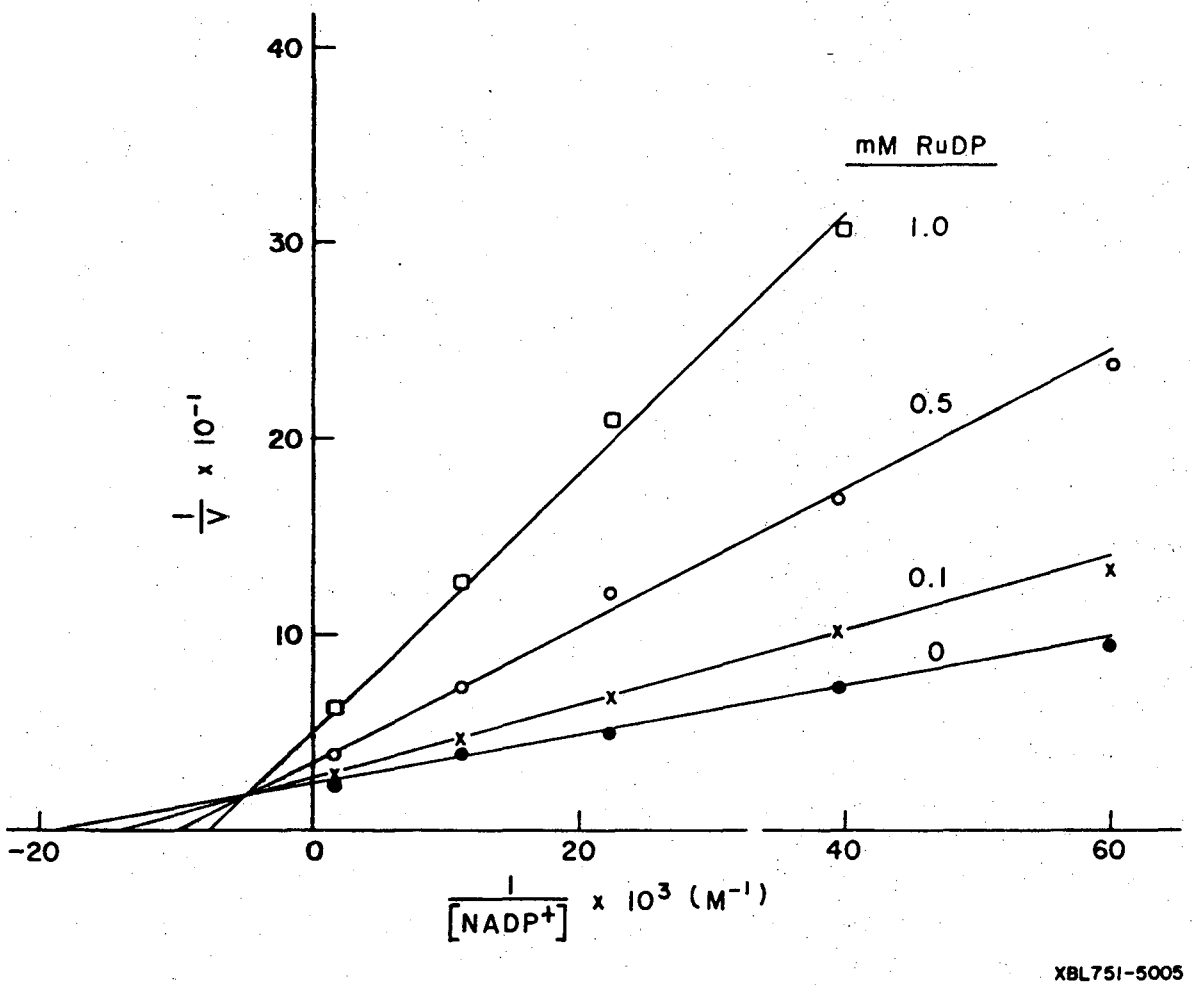
40
30
20
10
-20
0
20
40
60
mM RuDP
1.0
0.5
0.1
0
$\frac{1}{V} \times 10^{-1}$
$\frac{1}{[NADP^+]} \times 10^3 \ (M^{-1})$
XBL751-5005

Fig. 2

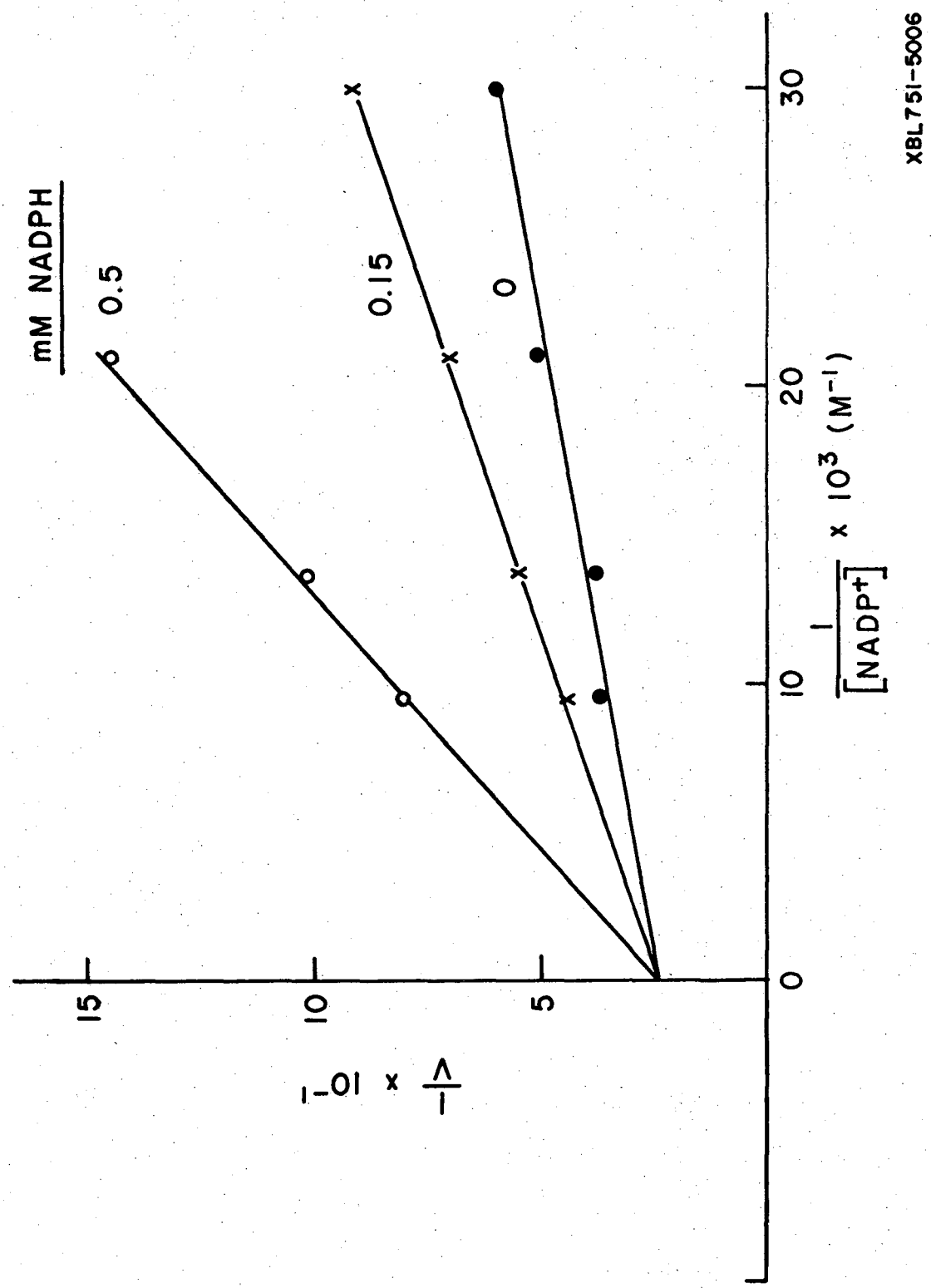
mM NADPH
0.5
0.15
0
15
10
5
0
10
20
30
$\frac{1}{V} \times 10^{-1}$
$\frac{1}{[NADP^+]} \times 10^3 (M^{-1})$
XBL751-5006

Fig. 3

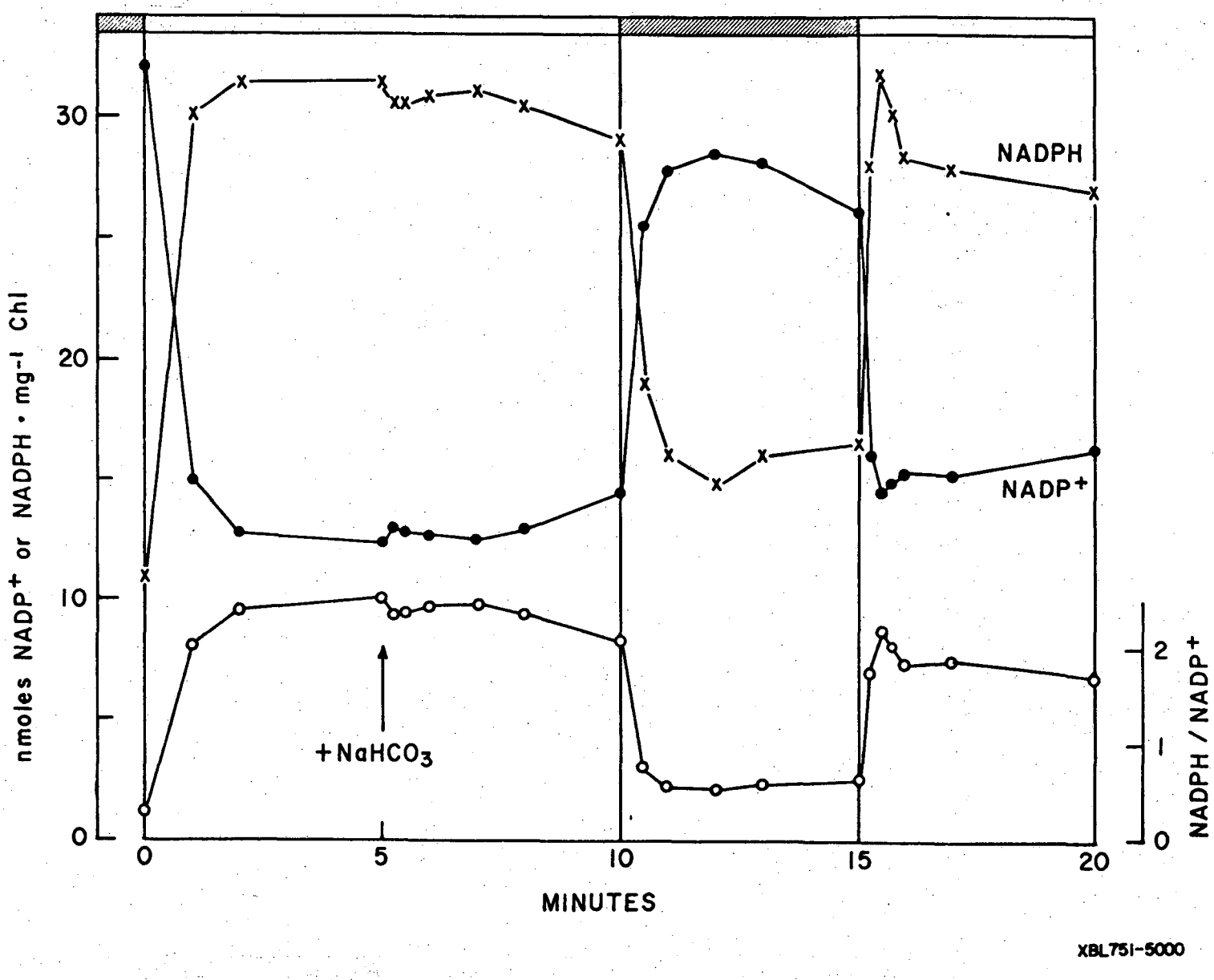
nmoles NADP+ or NADPH • mg-1 Chl
30
20
10
0
NADPH
NADP+
+NaHCO3
0
5
10
15
20
MINUTES
2
1
0
NADPH / NADP+
XBL751-5000

Fig. 4

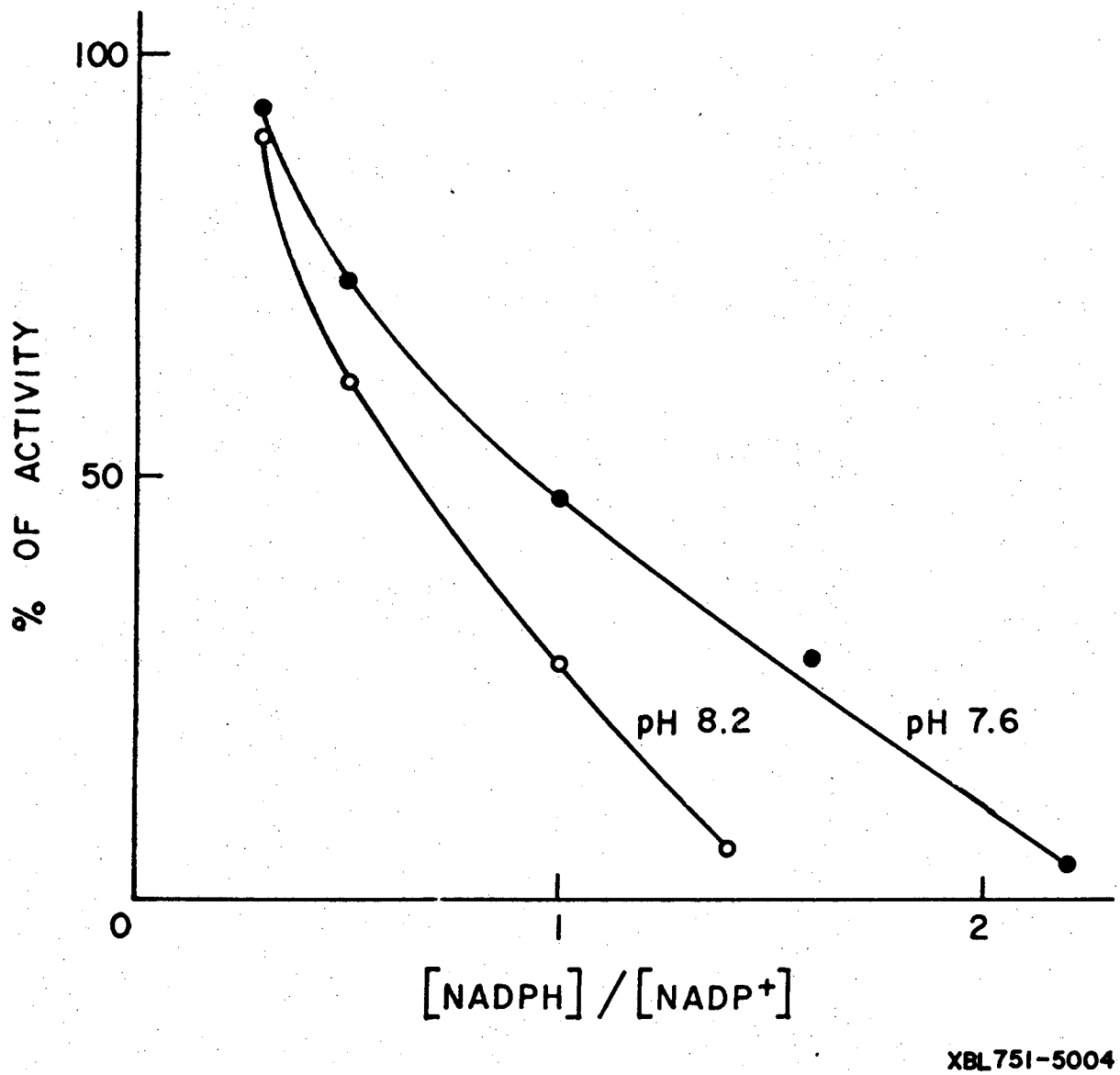

Fig. 5

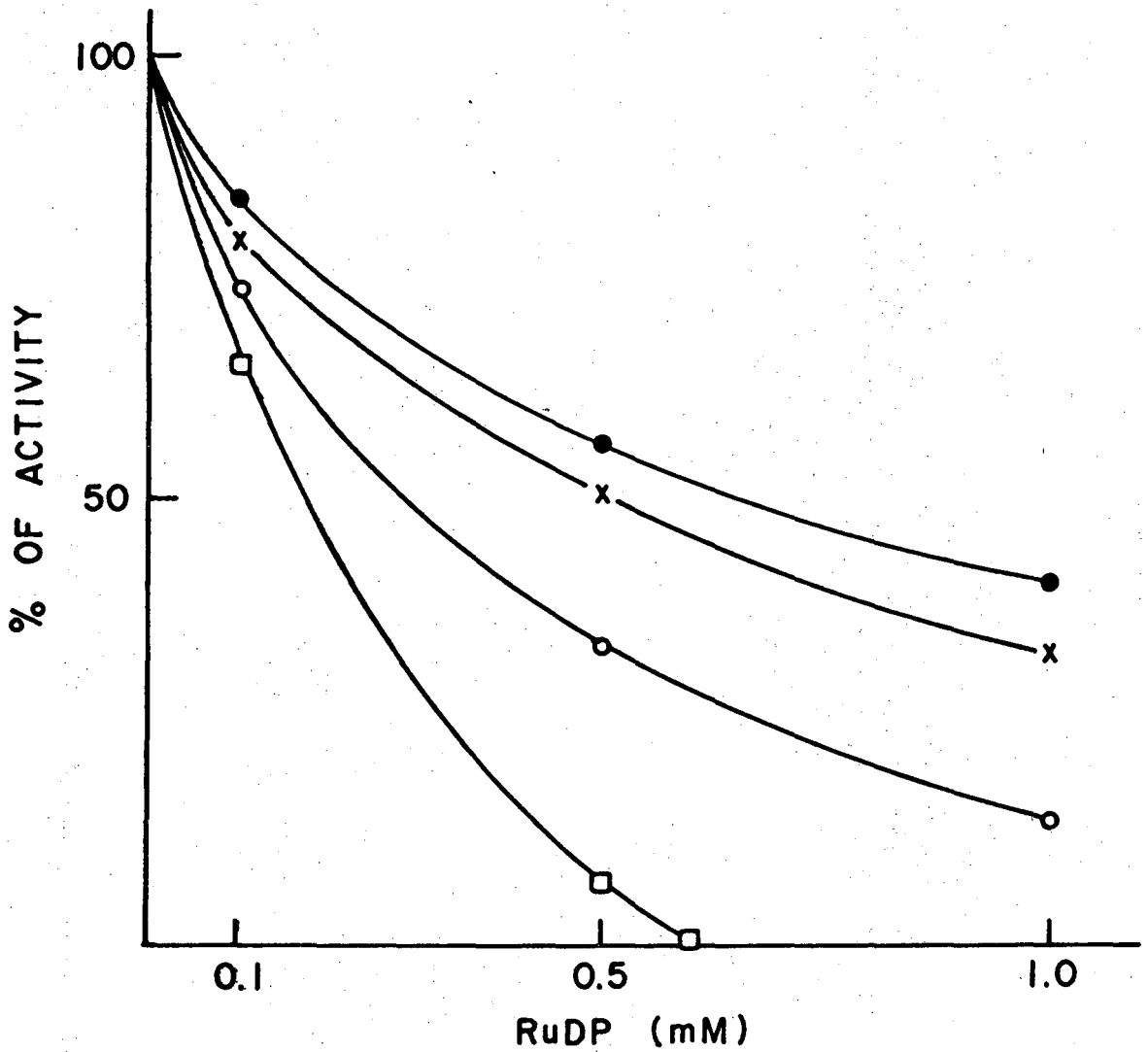

XBL751-5001

Fig. 6

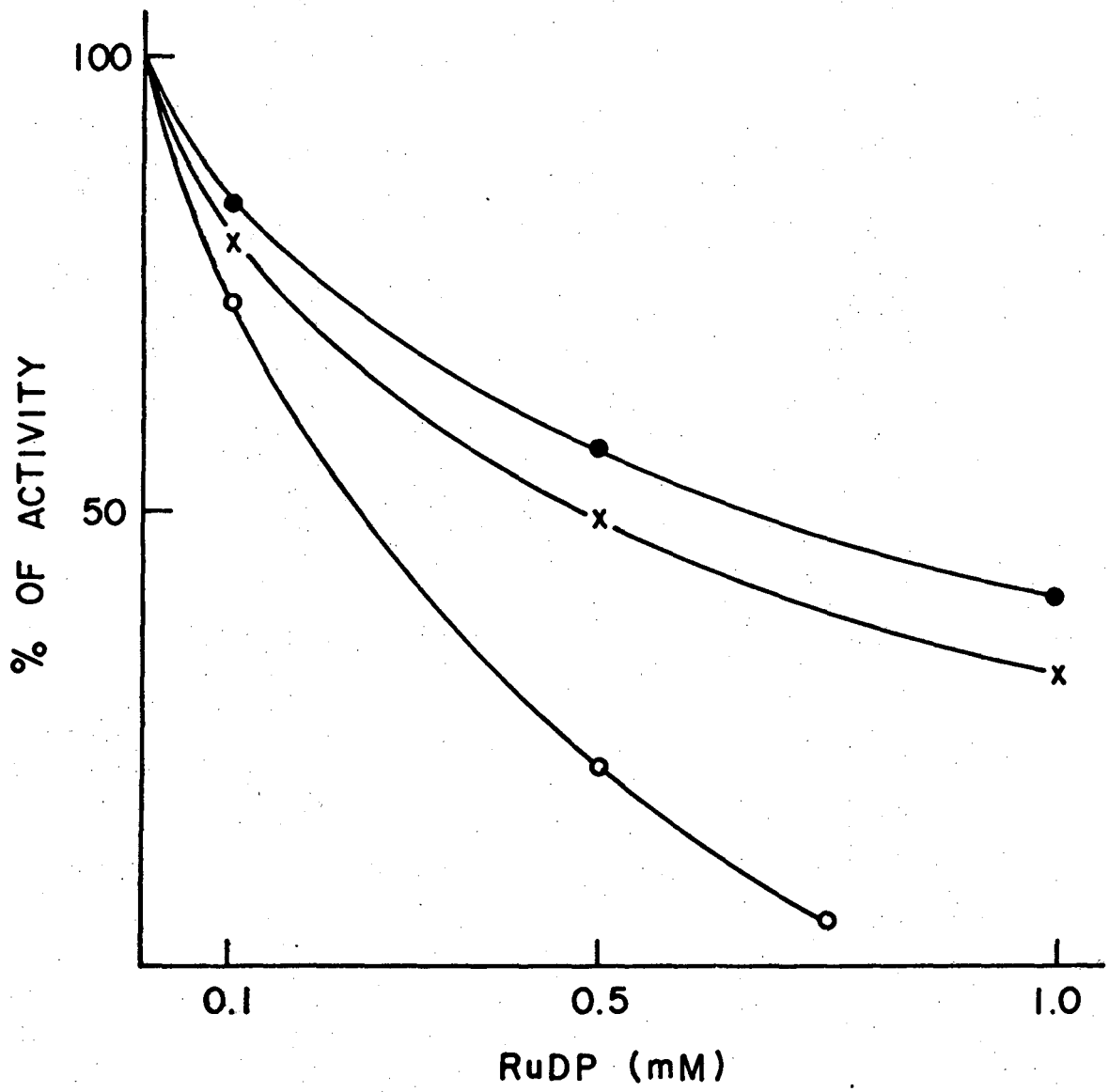

XBL751-5003

Fig. 7

0 0 0 0 4 3 0 1 5 1 2

LEGAL NOTICE

This report was prepared as an account of work sponsored by the United States Government. Neither the United States nor the United States Atomic Energy Commission, nor any of their employees, nor any of their contractors, subcontractors, or their employees, makes any warranty, express or implied, or assumes any legal liability or responsibility for the accuracy, completeness or usefulness of any information, apparatus, product or process disclosed, or represents that its use would not infringe privately owned rights.

TECHNICAL INFORMATION DIVISION
LAWRENCE BERKELEY LABORATORY
UNIVERSITY OF CALIFORNIA
BERKELEY, CALIFORNIA 94720